

Explainable machine learning for modelling of net ecosystem exchange in boreal forest

Ekaterina Ezhova^{1,*}, Topi Laanti^{2,*}, Anna Lintunen³, Pasi Kolari¹, Tuomo Nieminen¹, Ivan Mammarella¹, Keijo Heljanko^{2,4}, and Markku Kulmala¹

¹INAR/Physics, University of Helsinki

²Department of Computer Science, University of Helsinki

³INAR/Agricultural and Forest Sciences, University of Helsinki

⁴Helsinki Institute for Information Technology HIIT

*These authors contributed equally to this work.

Correspondence: Ekaterina Ezhova, ekaterina.ezhova@helsinki.fi

Abstract. There is a growing interest in applying machine learning methods to predict net ecosystem exchange (NEE) based on site information and climatic variables. ~~In case of successful performance, it could give an excellent opportunity for gapfilling or upscaling, i.e., extrapolation of results to times and sites for which direct measurements are unavailable. There exists already quite an extensive body of research covering different seasons, time scales, number of sites, input variables (features), and~~
5 ~~models.~~ We apply four machine learning models (Cubist, Random Forest, averaged Neural networks and Linear regression) to predict the NEE of boreal forest ecosystems based on climatic and site variables. We use data sets from two stations in the Finnish boreal forest (southern site Hyytiälä and northern site Värriö) and model NEE during the peak growing season and the whole year. ~~Using Explainable Artificial Intelligence For Hyytiälä, all nonlinear models demonstrated similar results with~~
10 ~~$R^2=0.88$ for the peak growing season and $R^2=0.90$ for the whole year. For Värriö, nonlinear models gave $R^2=0.73-0.76$ for the peak growing season; whereas Random Forest and Cubist with $R^2=0.74$ were somewhat better than averaged Neural networks with $R^2=0.70$ for the whole year. Using explainable artificial intelligence~~ methods, we show that the most important input variables during the peak season are photosynthetically active radiation, diffuse radiation ~~and vapour pressure deficit, whereas~~
15 ~~on the whole year scale, vapour pressure deficit, and vapor pressure deficit (or air temperature), whereas, on the whole-year scale, vapor pressure deficit (or air temperature)~~ is replaced by soil temperature. ~~When the data sets from both stations were~~
20 ~~mixed, soil water content, the only variable clearly different between Hyytiälä and Värriö data sets, emerged as one of the most important variables, but its importance diminished when input variables labeling sites were added.~~ In addition, we analyze the dependencies of NEE on input variables against the existing theoretical understanding of NEE drivers. We show that even though the statistical scores of some models can be very good, the results should be treated with caution, especially when applied to upscaling. In the model setup with several interdependent variables ubiquitous in atmospheric measurements, some models display strong opposite dependencies on these variables. This behavior might have adverse consequences if models are applied to the data sets in future climate conditions. Our results highlight the importance of ~~Explainable Artificial Intelligence~~
explainable artificial intelligence methods for interpreting outcomes from machine learning models, particularly when a set containing interdependent variables is used as a model input.

1 Introduction

25 Forests play an important role in the global carbon cycle because they remove carbon from the atmosphere through photosynthesis and store it in the wood biomass and forest soil. Recent studies suggest that in the past several decades, the net carbon uptake of the boreal forest has been increasing and that of the tropical forest decreasing, making the boreal forest the largest terrestrial carbon sink on the planet (Tagesson et al., 2020). The dynamics of the forest carbon cycle and its interaction with various climatic drivers are generally well-understood; however, the complex responses of forests to climate change and their potential to mitigate its impacts keep boreal forests at the forefront of multidisciplinary research. This ongoing interest spans from observational studies to global modeling efforts (Artaxo et al., 2022; Petäjä et al., 2022; Kulmala et al., 2020, 2023; Tang et al., 2023). There is a growing need for more accurate models of carbon fluxes, providing reliable results in warming climate conditions (Kämäräinen et al., 2023). Hence, suitable models must correctly capture current carbon cycle dynamics using commonly measured ecosystem-level data and give reasonable predictions for, e.g., future higher temperatures. In other words, the models' performance should be adequate in the range of values currently underrepresented in the data sets.

In addition to traditional process-based models (Launiainen et al., 2022; Junttila et al., 2023), the use of machine learning (ML) models have become ubiquitous. ML models play an important role in providing an alternative for the hypothetic-deductive modeling approach, i.e., an inductive approach. This means no prior assumptions are made about the data, which is modeled with a purely empirical model with a general function class. Currently, there is plenty of carbon flux data available from the FLUXNET database, as well as extensive meteorological reanalysis data sets or measurements of many different variables directly from research stations. Data availability has boosted the application of data-intensive ML methods to carbon flux modeling (Dou and Yang, 2018; Zeng et al., 2020).

Using ML, the functional relationship between carbon flux (net ecosystem exchange, gross primary production or respiration) and the site and climatic variables, including radiation, meteorological and biospheric input parameters, can be obtained. There exists plenty of literature featuring the ML approach to quantify different components of the carbon cycle using site and climatic variables as input (Dou and Yang, 2018). In many studies (Cai et al., 2020; Wood, 2021; Zhu et al., 2023; Zeng et al., 2020), researchers identify 'the best model' which reproduces the carbon fluxes depending on available set of input parameters better than other models. Statistical accuracy metrics are typically used as a criterion for model assessment. Many different ML models have been tested, but Random ~~forest~~Forest has appeared particularly popular (Liu et al., 2021; Reitz et al., 2021).

50 However, these empirical machine learning models are often "black box" in the sense that the ~~weights~~parameters used by models to make the predictions can not be directly extracted from the model to provide a human understandable way to interpret them easily. The results, therefore, should be treated cautiously. Recently, Shirley et al. (2023) demonstrated with an example from Alaska that the boosted regression tree ML model gave inaccurate results in current and future carbon balance estimates at high latitudes. Increasing the data set by adding more stations from the same area improved the result for the current carbon sink. Still, future estimates were unreliable, ascribed to the fact that the data sets representing future conditions could not be used for model training.

In response to this need, various methods that attempt to make ML models more open and interpretable have emerged. They are called explainable artificial intelligence (XAI) methods (Dwivedi et al., 2023). With XAI techniques, researchers can explore and analyze the factors that influence the model outcomes, making it easier to interpret the results and enhance the utility of ML approaches, e.g., in the context of carbon cycle research.

In the present study, we model boreal forest NEE with subhourly time resolution, using an extensive set of input variables from two research stations at different latitudes: Hyytiälä at 61°51'N and Värriö at 67°46'N. Using the same time resolution, we use different data sets considering separately the peak growing season (defined as the period of maximum photosynthetic activity of an ecosystem) and the whole year. One of the two data sets is divided into pre- and post-thinning data periods because the thinning of a forest (i.e. cutting down the share of trees ~~in a forest is cut down~~) significantly impacts not only the NEE, but also many site variables. ↪

We expect an ML model to learn differently depending on the seasonality of the time series used for model training. For example, diffuse radiation is an essential input variable for photosynthesis on a subhourly scale during the peak growing season because ecosystem photosynthesis is enhanced under higher diffuse radiation conditions due to better light use efficiency (Gu et al., 2002; Ezhova et al., 2018). In winter, this effect is missing, which might make diffuse radiation not as crucial variable for the model trained on the whole year data set. Instead, other input variables, such as air or soil temperature, can be relevant when focusing on the seasonal cycle of carbon fluxes (Kolari et al., 2009). Moreover, besides time-related factors, a spatial factor represented by latitude is also expected to affect the model buildup. The first aim of this study is to analyze how ML models treat input variables related to temporal (peak season vs whole year) and spatial variability.

The second aim is to use different ML models to understand how the best model's outcome compares to what we know from process understanding of the carbon fluxes' dynamics. In addition to that, we compare different ML models and check if all of them reproduce CO₂ flux dynamics robustly, if they tend to choose the same important input variables, and if dependences on these variables are similar between the models.

Finally, we combine data sets from the two latitudes, include data from a post-thinning period in Hyytiälä, and use XAI to understand how the models perform on this mixed data set. We introduce additional variables (the site variables) distinguishing between the sites and model NEE with and without these variables.

In this study, we have several research goals: 1) compare the ML models' performance for two ecosystems from different latitudes but with the same main tree species using accuracy metrics and XAI (with a linear regression model as a baseline); assess the reliability of results based on the robustness of their reproduction by different models; 2) analyze the shift in the choice of model variables and their general performance depending on the seasonality (i.e., peak growing season or the whole year) and latitude; 3) study how combining the data sets from the two studied forest ecosystems at different latitudes and including post-thinning data affects model results.

Table 1. Amount-Summary of observations data sets: time periods and date-ranges-number of each data-set observations.

Site and case	Dates	<i>N</i> obs.
Hyytiälä, all-season whole year	07/2008 - 09/2018	39096
Hyytiälä, peak season	Jul-Aug (2008 - 2018)	11730
Post-thinned Hyytiälä, all-season whole year	02/2019 - 05/2021	11690
Post-thinned Hyytiälä, peak season	Jul-Aug (2019 - 2020)	1376
Värriö, all-season whole year	05/2013 - 10/2019	26138
Värriö, peak season	Jul-Aug (2015 - 2019)	7172

2 Materials and methods

2.1 Stations and data sets

90 We used atmospheric observations from the SMEAR II station in Hyytiälä, Finland (Hari and Kulmala, 2005) and SMEAR I station in Värriö, Finland (Hari et al., 1994). The stations are located in boreal forest in central Finland (Hyytiälä: 61°51'N, 24°17'E, 80 m a.s.l.) and in Finnish subarctic region (Värriö: 67°46'N, 29°36'E, 180 m a.s.l.). The mean annual air temperature is 3.5°C in Hyytiälä and -0.5°C in Värriö (source: ICOS database). The mean annual precipitation in Hyytiälä is 710 mm, and in Värriö, it is 601 mm. Forest stands at both sites are dominated by 60-65-year-old Scots pines (*Pinus sylvestris* L.).

95 However, the average tree height differs, being ca. 19.9 m at SMEAR II and 10 m at SMEAR I, as measured in 2023. The forest canopy at SMEAR II is closed, and at SMEAR I, it is open. Both sites are part of the Integrated Carbon Observation System (ICOS) and Integrated European Long-Term Ecosystem, critical zone, and socio-ecological Research (eLTER) networks. ~~ICOS provides high-quality data on greenhouse gas concentrations and carbon fluxes between the atmosphere, Earth, and oceans. Conversely, eLTER focuses on long-term, site-based ecosystem research across various European locations. Each site contributes by measuring, meaning continuous observations of~~ carbon fluxes and ~~studying ecosystems, respectively other~~ ecosystem parameters. Meteorological variables and radiation levels are also routinely measured at the stations. The data is publicly available to download from the SmartSMEAR database (<https://smear.avaa.csc.fi/>, accessed September 2022; latest updated data sets can be found at <https://etsin.fairdata.fi/datasets/SmartSMEAR>).

100

Data from Hyytiälä was divided into two separate data sets, pre-thinning, referred to just as Hyytiälä data (prior to 2019), and post-thinning (post 2019), referred to as post-thinning Hyytiälä data. The separation is due to the thinning of the forest at Hyytiälä station in 2019, which involved the removal of smaller trees from the forest understory, and additional thinning (from below) conducted from January to March 2020. In the thinning, 30% of tree basal area was removed (Aalto et al., 2023), which significantly changed NEE due to the decrease of biomass. The data set thus had too large differences to be treated as a direct continuation of the pre-thinning data set. The amount of data points and the ~~dates-time intervals~~ for each data set can be seen

105

110 in Table 1.

The data used in this study was at a 30-minute ~~measurement~~-interval. The ~~higher-high~~ frequency enables a more detailed study of the daily cycle of NEE. It allows for the analysis of the impact of such variables that affect the ecosystem processes on a short time scale, such as the impact of changes in radiation on photosynthesis. Raw data for the target variable (NEE) being modeled with the machine learning models is first captured using eddy covariance technique (Aubinet et al., 2012) and then processed to NEE using the EddyUH software (Mammarella et al., 2016). Negative NEE corresponds to the ecosystem acting as a net carbon sink, while positive corresponds to the ecosystem acting as a net carbon source. We model NEE using meteorological variables such as air temperature, soil temperature, solar radiation, relative humidity, and soil moisture content. LAI is not used here as its seasonal variability in the chosen period is relatively small (Hyytiälä - about 30%, Värriö - 20%), which translates to below 10% change in canopy light interception and roughly the same percentage in GPP. For some input variables, minor differences exist in how the data is measured at the two stations (e.g., soil moisture is from slightly different depths). The data used was non-gapfilled to avoid the influence of models typically used for gapfilling. At Hyytiälä, photosynthetically active radiation (PAR) was not measured before 2009, and we used global radiation multiplied by the PAR quantum efficiency of $2 \mu\text{mol s}^{-1} \text{W}^{-1}$ (Ross and Sulev, 2000; Ezhova et al., 2018) to calculate missing values of PAR. ~~A table of all variables used can be seen~~ All variables used are listed in Table 2.

In the pre-processing of the data, time points that contained missing values of any studied input variable were discarded. Also, all rows where the PAR value was less than $10 \mu\text{mol s}^{-1} \text{m}^{-2}$ were filtered out due to the interest being solely on modeling daytime NEE. We calculated the diffuse fraction:

$$F_{dif} = \frac{\text{PAR}_{dif}}{\text{PAR}}, \quad (1)$$

and vapor pressure deficit (Monteith and Unsworth, 2013):

$$\text{VPD} = e_s - e_a, \text{ where } e_s = 611 \exp\left(\frac{17.27T_{air}}{237.7 + T_{air}}\right), e_a = e_s \frac{\text{RH}}{100}. \quad (2)$$

In eq. (2), T_{air} is in units [$^{\circ}\text{C}$] and e_s , e_a are in units [Pa].

The machine learning models were trained in two sets of four ~~where setups~~ (Table 3), and the results within a set ~~are were~~ compared against each other. For both sets, four different machine learning models were trained for all of the four cases ~~for meaning~~ total of thirty-two models trained. In the first set, ~~models for pre-thinned Hyytiälä and Värriö, models for both all season (data consisting of entire year)~~ data representing entire year and peak growth season (July and August) were trained using ~~only~~ data from either pre-thinned Hyytiälä or Värriö. In the second set, models were trained by combining the ~~different datasets data from two sites~~ into a single mixed dataset and then training them with and without ~~a label that denotes variables that denote~~ from which site the data originates from ('Värriö', 'Hyytiälä' for Hyytiälä pre-thinned, 'HyytiäläT' for Hyytiälä ~~thinned~~ both post-thinned). Similarly to Set 1, setups included entire year and peak growing season. A table summary of the configurations for ~~the all~~ experiments can be seen in Table 3.

In all cases, the data was split into training and test data, where training data was used to train the models, while test data was used to evaluate the models' performance. For modeling NEE for pre-thinned Hyytiälä and Värriö, 75% of their respective

Table 2. List of input variables used for model training.

Abbreviation	Name	Units	Notes
PAR	Photosynthetically Active Radiation	$\mu\text{mol s}^{-1} \text{m}^{-2}$	Hyytiälä: Measured at 18 m height (radiation tower 12/2009-2/2017) or 35 m height (35 m tower 2/2017-). Värriö: - .
PAR_{dif}	Diffuse PAR	$\mu\text{mol s}^{-1} \text{m}^{-2}$	Hyytiälä: Measured at 18 m height (radiation tower 12/2009-2/2017) or 35 m height (35 m tower 2/2017-). Värriö: - .
F_{dif}	Diffuse Fraction	-	$F_{dif} = \frac{PAR_{dif}}{PAR}$
AirTemp	Air Temperature	°C	Hyytiälä: Measured at 33.6 m height. Värriö: 9 m
SoilTempA	Soil Temperature	°C	Hyytiälä: Measured 2-5 cm depth in the mineral soil). Värriö: 5cm.
SoilTempB	Soil Temperature	°C	Hyytiälä: Measured 22-29 cm depth in the mineral soil (Only in Hyytiälä)
VPD	Vapor Pressure Deficit	Pa	Formula listed (2) , section 2.1
SoilWatCont	Soil Water Content	%	Hyytiälä: 26-36 cm depth in the mineral soil. Värriö: - .
RH	Relative Humidity	%	Hyytiälä: Measured at 16 m height (4/1998-1/2017) or 35 m height (2/2017-). Värriö: 2m.
FricVel	Friction Velocity	m/s	Hyytiälä: Measured at 24 m height, 27 after 2019. Värriö: Measured at 16.6 m height

data was used for training the model, while the rest was used as the test data to evaluate the model performance. In case of the mixed model, 80% of the each respective data set was used to train the model.

145 2.2 Machine learning models

To ensure robustness and reduce potential biases, we validate our findings across four distinct ML models, aiming to identify consistent patterns or insights and provide an overall picture of how well the models can use this data to predict NEE. Applying several models to the same data set provides a context on what input variables are consistently considered important across different models. The four models used were Cubist (Quinlan, 1992), Random Forest (Breiman, 2001), [avNNet-Averaged neural](#)
150 [network](#) (Kuhn, 2008), and basic Linear Regression (Kutner et al., 2004). All were implemented in R (v. 4.3.0: <https://www.r-project.org/>) using R's "caret" library (v. 6.0.94: <https://github.com/topepo/caret/>). Linear Regression served as the baseline model, while the other models were chosen due to their proven competence in solving various regression problems (Fernández-Delgado et al., 2019).

Table 3. Overview of the training configurations for ML models across different datasets.

Set	Site/Data - Period - <u>Setup</u>	Description
Set 1	Hyytiälä All	Models trained on the data from pre-thinned Hyytiälä, entire years
	Hyytiälä Peak	Models trained on the data from pre-thinned Hyytiälä, peak growing seasons
	Värriö All	Models trained on the data from Värriö, entire years
	Värriö Peak	Models trained on the data from Värriö, peak growing seasons
Set 2	All Site-All - <u>Without Site</u>	Models trained on the mixed data set from both sites, including post-thinned Hyytiälä, entire years, no site labels
	All Site-All (Label) - <u>With Site</u>	Models trained on the mixed dataset from both sites, including post-thinned Hyytiälä, entire years, sites labels included
	All Site-Peak - <u>Peak Without Site</u>	Models trained on the mixed dataset from both sites, including post-thinned Hyytiälä, peak growing seasons, no site labels
	All Site-Peak (Label) - <u>Peak With Site</u>	Models trained on the mixed dataset from both sites, including post-thinned Hyytiälä, peak growing seasons, site labels included

Random ~~Forest~~-forest (RF) is a popular model that has been used in previous research (Cai et al., 2020; Liu et al., 2021; 155 Abbasian et al., 2022; Zhu et al., 2023) due to its ease of use, high accuracy, and robustness. It is an ensemble model that uses the averaged output of random regression trees (Fernández-Delgado et al., 2019) by training different regression trees on different subsets of the data. The final prediction is the average result of the different tree predictions. The algorithm is quite robust as the different trees are trained with the different subsets of the training data. The randomForest library (Liaw and Wiener, 2002) implements the regression algorithm of ~~Random Forest~~-RF used in this study.

160 Cubist is one of the best-performing regression models (Fernández-Delgado et al., 2019) across multiple types of data sets (i.e., type and size of data). Like ~~Random Forest~~-RF, it is created from multiple individual regression trees, where each terminal leaf contains a smoothed linear regression model for prediction (Zhou et al., 2019). It creates a series of "if-then" rules that can be considered the branches of a tree, while the leaves are an associated multivariate linear model. The corresponding model is used to calculate the final predicted value as long as the set of covariates satisfies the conditions of the corresponding 165 rule. Cubist also uses boosting with its training committees, which creates a series of trees with different weights and nearest-neighbors search to adjust the predictions better.

Model Averaged Neural Networks (avNNet) is a single hidden layer feed-forward neural network characterized by ~~their~~ its 170 architecture and training approach. The network consists of interconnected neurons arranged in layers, with the final layer outputting the prediction (Ripley, 2007). During the training phase, initial weights, which influence predictions, are randomly assigned. These weights are then iteratively updated, enabling the network to capture nonlinear relationships. Given the randomness in predictions due to these initial weight assignments, avNNet constructs multiple neural network models and aver-

ages their results. This averaging process promotes a more robust and stable prediction by minimizing the impact of any single model's randomness.

175 The basic multivariate Linear Regression ([LinRegr](#)) is used as a baseline to understand how much impact and improved results more advanced models can provide. ~~Linear regression~~ [LinRegr](#) finds a linear relationship between the independent and dependent variables determined by minimizing the sum of the squared differences between the predicted and the actual values (Hastie et al., 2009).

2.3 Cross-validation framework, ~~Hyperparameter~~ [hyperparameter](#) tuning and validation metrics

180 K -fold cross-validation is a resampling method for validating model efficiency, which ~~ögenerally~~ [generally](#) results in less biased models (Jung, 2018). K -fold cross-validation method shuffles the data set randomly and splits it into K groups or folds. First, each fold is taken as a holdout, while the model is fit on the rest of the folds, and then the model is evaluated on the holdout set. The score is retained, and the model is discarded. In repeated K -fold cross-validation, this process is done R times on different splits. [K-Fold cross-validation also effectively prevents model overfitting, where a machine learning model has learned to model the inherent noise of a dataset, to a point where it fails to model for points not included in the training dataset \(Berrar, 2019\).](#)

185 During the model training, repeated K -fold cross-validation was used with Caret librarys (Kuhn, 2023) grid hyperparameter search. This method trains and evaluates a model using all possible combinations of specified hyperparameter values to identify the combination that yields the best model performance. It was used to tune the models' hyperparameters and configuration settings that are external to the model and can be adjusted to optimize performance. Values $R = 5$ repeats and $K = 10$ folds were used to fit each model. The tuned hyperparameters can be seen in Table 4. The train and test data as well as the folds of the K -fold cross-validation were split using a predetermined random split to ensure repeatability. However, due to technical limitations, in-depth hyperparameter tuning was not used on the models that contained data from all sites. Instead, hyperparameters based on the results from the single-site models were used.

195 In evaluating the performance of our machine learning models, we primarily relied on two key metrics to assess the models' goodness of fit: the coefficient of determination (R^2) and the root mean squared error (RMSE). RMSE measures the differences between the values predicted by a model and the actual values and provides an understanding of the magnitude of error the model might make in its predictions. A lower RMSE indicates a better fit to the data, implying that the model's predictions are more precise. The models' hyperparameters were tuned specifically based on the RMSE score.

200 [In addition, each model was trained on five different data splits to account for variability and reduce the influence of any single fortunate or unfortunate split on the results. The performance metrics, \$R^2\$ and RMSE, were averaged across these splits to ensure a robust and reliable assessment of model performance.](#)

2.4 Explainable AI Methods

As machine learning models have been used more in research and industry, the demand for more transparent and interpretable models has grown (Dwivedi et al., 2023). As ~~the~~ model accuracy has risen, so has ~~the~~ model complexity. The highly accurate

Table 4. List of the final model hyperparameters with their respective values for each [data-setmodelling_setup](#). Values [correspond-of-parameters-are-listed-in-the-following-order-corresponding](#) to different [sitesetups](#): Hyttiälä All, Hyttiälä Peak, Värriö All, Värriö Peak, [All-Site-Models-Mixed data sets](#) with site label and [All-Site-Models-Mixed data sets](#) without [Site-site](#) label.

Method	Hyperparameter	Description	Values
Cubist	committees	Number of committees (models) to be fitted.	100, 90, 100, 100, 100, 100
	neighbors	Number of nearest neighbors used in prediction.	9, 9, 6, 3, 9, 6
Random Forest	mtry	Number of variables sampled at each split.	3, 3, 6, 2, 13 , 9 , 11 , 8
	min node size	Minimum size of terminal nodes (leaves).	5, 5, 5, 5, 5, 5
avNNet	size	Number of units in the hidden layer(s).	13, 13, 13, 13, 13, 13
	decay	Weight decay parameter for regularization.	0.1, 0.1, 0.1, 0.1, 0.1, 0.1
	bag	Boolean flag for using bootstrap aggregating (bagging).	False, False, False, False, False, False

205 and complex models have many hyperparameters that can not be made human-understandable. To be [trustabletrustworthy](#), the ML model must produce interpretable or transparent results. Relying on unexplained or inaccurate predictions can lead to critical errors. Accuracy metrics do not always portray the true prediction capability of a model, so it is vital to critically evaluate the results against existing knowledge or theories. XAI methods aim to provide machine learning models and methods that enable users to better understand, analyze, and evaluate the models' decision-making.

210 In this study, we used two XAI methods: permutation feature importance and accumulated local effect (ALE) plots (Molnar, 2020). They provide insight into how the input variables affect a model's output. Both are model-agnostic global methods, meaning they can be used regardless of the selected model and provide interpretations on the data set as a whole rather than individual points (Molnar, 2020). Both of these methods were implemented using R's "iml" library (v.0.11.1: <https://github.com/christophM/iml/>, Molnar et al. (2018)).

215 2.4.1 Permutation Feature Importance

Permutation feature importance is a method that aims to measure the increase in the prediction error of a model after the input variables (features) are permuted. In permutation feature importance, the relationship between a specific input variable and the variable the model tries to predict is deliberately disrupted to understand how the models' prediction accuracy is affected (Molnar, 2020). If an input variable is important, randomly rearranging its values increases the model error, as the
 220 model then relies on that specific input variable for an accurate prediction. Trained model is denoted as f , input variable matrix as \mathbf{X} , target vector as \mathbf{y} , and error measure $L(\mathbf{y}, f(\mathbf{X}))$. The algorithm works as follows:

1. Estimates the original model error $e = L(\mathbf{y}, f(\mathbf{X}))$
2. For each input variable with index $i \in \{1, \dots, p\}$, where p is the total number of input variables, the following is done:

- 225 2.1 Generates a permuted input variable matrix $\hat{\mathbf{X}}$ by permuting input variable i in the data \mathbf{X} , which breaks the association between input variable i and the true outcome \mathbf{y} .
- 2.2 Estimates the error caused by the permutation by predicting with it $\hat{e} = L(\mathbf{y}, f(\hat{\mathbf{X}}))$.
- 2.3 Calculates permutation input variable importance as quotient $Imp_i = \hat{e}/e$.
3. Sorts input variables by descending Imp .

230 Only test data is used to calculate the permutation feature importance. Assessing feature importance using the training data might result in too inflated scores due to a model overfitting on training data. That said, the features with very high scores might not be as important for making accurate predictions on new, unseen data. [As with the metrics \$R^2\$ and RMSE, the Permutation Feature Importance was calculated on multiple different datasplits to ensure robustness of the results.](#)

2.4.2 ALE Plots

235 Accumulated local effect (ALE) plots describe how input variables influence the prediction of a machine learning model on average (Molnar, 2020). ALE reduces a complex machine learning function to a function that depends on only one, as in our case, or two input variables and visualizes the effects between a selected variable and the prediction of the target variable of a machine learning model. The idea is to remove the unwanted effects of other input variables, take partial derivatives (local effects) of the prediction function with respect to the feature of interest, and integrate (accumulate) them with respect to the same feature.

240 The value of ALE at a certain point can be thought of as the effect of the selected variable at a specific value compared to the average prediction made on the data. To calculate ALE value for input variable s at point $x \in [\min(\mathbf{x}_s), \max(\mathbf{x}_s)]$, with \mathbf{x}_s being the vector of this variables values, the input variable values \mathbf{x}_s are divided into K intervals, where the start of the first interval is the lowest value $z_0 = \min(\mathbf{x}_s)$, and the differences of predictions between the sequential intervals is calculated. While the exact ALE formula requires a model with a derivative, an approximate version is used here that is more widely
245 adopted and works for models without a derivative. Initially, an uncentered effect is computed:

$$\bar{f}_{s,ALE}(x) = \sum_{k=1}^{k_s(x)} \frac{1}{n_s(k)} \sum_{i: x_s^{(i)} \in [z_{k-1,s}, z_{k,s}]} \left[f(z_{k,s}, \mathbf{x}_{-s}^{(i)}) - f(z_{k-1,s}, \mathbf{x}_{-s}^{(i)}) \right].$$

The input variable of interest is replaced with grid values \mathbf{z} , where the grid values represent the edges of the intervals. The interval index an input variable value $x \in \mathbf{x}_s$ falls in is denoted as $k_s(x)$, while $n_s(k)$ denotes the number of observations inside the k -th interval of \mathbf{x}_s . A single data point is denoted as $\mathbf{x}^{(i)} = (x_s^{(i)}, \mathbf{x}_{-s}^{(i)})$, where $x_s^{(i)}$ denotes the i -th value for the selected input variable, and $\mathbf{x}_{-s}^{(i)}$ is the vector of all the other features of a single data point that are kept constant. The ML predicting
250 function is denoted as f .

The differences between the predictions $f(z_{k,s}, \mathbf{x}_{-s}^{(i)}) - f(z_{k-1,s}, \mathbf{x}_{-s}^{(i)})$ are the effect that the input variable s has for an individual data point to predicting the dependent variable (NEE in our case) when using the upper and lower values of an

certain interval. The sum $\sum_{i: x_s^{(i)} \in]z_{k-1,s}, z_{k,s}]}$ adds up the effects of all instance within an interval $x_s^{(i)} \in]z_{k-1,s}, z_{k,s}]$. This is then divided by the number of observations in this interval $n_s(k)$ to obtain the average difference of the predictions of this interval. The sum $\sum_{k=1}^{k_s(x)}$ accumulates the average effects across all intervals, meaning that the uncentered ALE of an input variable of interest is accumulated by all its previous intervals. After that, the effect is centered, making the mean effect zero:

$$f_{s,ALE}(x) = \bar{f}_{s,ALE}(x) - \frac{1}{n} \sum_{i=1}^n \bar{f}_{s,ALE}(x_s^{(i)}).$$

The value of ALE can be thought of as the main effect of the input variable at a certain value compared to the average prediction of the data. ALE plot has the advantage that it generates valid interpretations even if the variables are correlated, an issue that persists in other methods that reduce a prediction function f to a function that depends on a single input variable such as PDP or M-plots (Molnar, 2020). As with permutation feature importance, only the test data set was used to reduce the chance of inflating scores due to a model overfitting on the training data set.

3 Results and discussion

3.1 NEE modelling for Hyttiälä and Värriö data sets

In this section, we report the results obtained with different models ~~for the two cases: Värriö data and pre-thinning conditions in from the Set 1 in Table 3 (pre-thinned Hyttiälä . The results are shown separately for the and Värriö,~~ whole year and ~~for the~~ peak growing season). First, we assess models' performance with routinely used accuracy metrics (R^2 ~~-coefficient of determination, and root-mean-squared-error, and~~ RMSE), visualize diurnal ~~/and~~ annual NEE cycles, and then use XAI methods. In each subsection, we start the discussion with the peak growing season results and continue with the ~~all-season-whole season~~ results.

3.1.1 Assessing model performance using accuracy metrics

Figs. 1 and 2 show coefficients of determination and RMSE, respectively, for all the models, two stations, ~~and trained on the data sets for the whole year and~~ the peak growing season, and the whole year (Set 1 in Table 3). In general, the models perform better if trained on the Hyttiälä data set compared to the Värriö data set, as seen from higher R^2 -coefficients. If the model is used on the training data set, the ~~R-coefficients~~ R^2 -coefficients and RMSE are somewhat better than when used on the test data set, as expected. This effect is especially pronounced for ~~Random Forest, reaching RF and Cubist models, which achieve high scores ($R^2 > 0.9$) in all cases on the training data, but also for Cubist(0.85),~~ largely because they are regression tree-based models that tend to produce overly optimistic results on the data they were trained on. These high training scores do not reflect Out-of-Bag (OOB) performance, which typically provides a more accurate estimate of the model's true predictive ability on the data it was trained on (Kuhn and Johnson, 2013), due to it not being available to use on all models. The difference between the train and test scores is larger for Värriö than for Hyttiälä. ~~Neural network and Linear models, as can be expected because Värriö data set is smaller (Zhang et al., 2023).~~ LinRegr and avNNet have almost identical scores on training and test data sets.

The difference in scores between the training and test data sets is called generalization error. In some cases, large generalization error points to overfitting, i.e., the model learns the training data set too well and then performs poorly on the test data set. We applied K-fold cross-validation to avoid overfitting when choosing hyperparameters; see subsection 2.3. Additionally, we tried different splits of the data into training and test data sets, which showed that the variation of the resulting R^2 -coefficients and RMSE was small (Fig. 1, 2). In addition, we obtained similar accuracy metrics on the test data sets using different nonlinear ML models, which also suggests that our results are robust. In what follows, the results are reported for the test data sets if not stated otherwise.

For the peak growing season, all four models perform well, including ~~linear regression~~ LinRegr, which is only slightly worse than the more complex models. For Hyytiälä, all nonlinear ML models give similarly high R^2 -coefficients, close to 0.9, and RMSE values almost do not differ between these models. For Värriö, RF is slightly better than other ML models, ~~demonstrating~~ ~~demonstrated by~~ both higher R^2 -coefficient and lower RMSE. Compared to Hyytiälä's ~~$R^2 = 0.88$~~ $R^2 = 0.87$, Värriö's R^2 -coefficient is ~~smaller, $R^2 \simeq 0.75$~~ ~~lower, $R^2 \simeq 0.70 - 0.74$~~ , which could be related to the ~~presence of a larger relative number~~ ~~higher share~~ of outliers in the data or a smaller ~~variability range of a range of the~~ predicted variable. The predictors vary within similar ranges in Hyytiälä and Värriö, whereas the predicted variable NEE has a larger value range in Hyytiälä compared to Värriö (corresponding to a weaker carbon sink in Värriö) because Värriö ecosystem is less productive. ~~Similar decrease in R^2 -coefficients for the cases when predicted variable had a smaller variability range was reported by Liu et al. (2021) and Abbasian et al. (2022).~~ ~~The~~ ~~It is also possible that the~~ difference in R^2 -coefficients could be because the ~~chosen available~~ predictors have a more significant effect on ~~the~~ forest carbon balance in Hyytiälä than in Värriö. A ~~big proportion of Värriö data comes from the dormant season, when the explanatory variables have virtually no effect, and the fluxes are near zero all the time. In addition, the temperature effect on NEE in Värriö could be more complicated than in Hyytiälä, with a stronger accent on a temperature history (Mäkelä et al., 2004); ecosystem response to temperature has a delay which is only partially accounted for here by the use of soil temperature as one of the input variables. It is also known that Värriö ecosystem responds weakly to cold spells during the growing season, making temperature dependence even more complex. Note that also decrease~~ ~~in R^2 -coefficients for the cases when the predicted variable had a smaller value range was reported by other ML studies, e.g., Liu et al. (2021) and Abbasian et al. (2022).~~ Also, for process-based models ~~experience difficulties in~~, reproducing carbon fluxes at ~~sites less productive forests~~ with low leaf area index ~~is challenging~~ (Mäkelä et al., 2019).

Scatter plots of measured vs. modeled data for training and test data sets are shown in Fig. 3 using one of the best performing models, RF. The lowest ~~values of NEE modelled NEE values~~ tend to be overestimated, and the ~~largest ones highest~~ underestimated. This is seen best in the training data sets (because they are much larger) deviating from 1:1 lines at the extremes of the data. ~~In that sense, higher scores of the training data sets should not be deceiving: a high correlation does not mean that the model values correspond perfectly to the measured values.~~ In Fig. 2, it is visible that RMSE values for Värriö are ~~smaller lower~~ than those for Hyytiälä, which means that Värriö values in Fig. 3 are closer to the best-fit lines. Still, ~~again~~, it does not mean that the model is better because the best-fit line of the measured vs. modeled data points is not 1:1. By high accuracy scores, the mean diurnal cycle of NEE within the peak growing season is almost perfectly reproduced by the RF model (Fig. 4) with slightly smaller standard deviations in the modeled than measured data.

In the case of the ~~all-season-whole-year~~ data sets, the performance of ~~linear-regression-LinRegr~~ drastically decreases when compared to the peak growing season data sets (Figs. 1, 2). This could be expected because, on the whole-year scale, NEE dependence on many variables becomes nonlinear. Especially for the Värriö data set, ~~linear-regression-scores-fall-LinRegr~~
320 ~~R^2 -coefficient falls~~ below 0.5, and RMSE increases by 40% compared to ~~the~~ nonlinear ML models, meaning that more complex models are needed and justified. Figs. 3 - 5 show scatter plots and annual daytime NEE cycle for Hyytiälä and Värriö. The same conclusions as for the peak growing season data sets apply here as the mean values were almost perfectly reproduced and extreme values missing. The models captured the essential features of the annual NEE cycle, including ecosystem spring and autumn phenological transitions (Fig. 5).

325 It is interesting to consider different models' performance for the same setup. Here we show an example for Hyytiälä ~~all-year data set-All setup~~ (Fig. 6). The test cases for all ~~nonlinear~~ ML models look similar. Note orange points (test RF) covering black points (training RF) illustrating the smaller RMSE for the training data set. ~~The linear model in Fig. 6. LinRegr~~ plot is more scattered, and the points are not organized along one line (in agreement with ~~previously~~ reported low R^2 -coefficients and high RMSE).

330 ~~Concerning-Compared to~~ other studies, Dou and Yang (2018) demonstrated that in modeling whole-year NEE of forest ecosystems, the R^2 -coefficients as high as 0.64-~~0.84~~-~~0.80~~ can be reached on the test data sets for separate ~~evergreen needleleaf forest~~ ecosystems. Our scores are within this interval for Värriö and significantly higher (0.90) for Hyytiälä. However, we used a different, more diverse set of input variables and modeled half-an-hour fluxes compared to daily fluxes in the study mentioned above. ~~On a similar data set (deciduous forest in Germany, summer time, half-an-hour resolution), Moffat et al. (2010) got~~
335 ~~$R^2 = 0.93$ and RMSE of $2.3 \mu\text{mol s}^{-1} \text{m}^{-2}$ using artificial neural network, which is close to Hyytiälä results.~~

3.1.2 ~~Feature importance and ALE~~

~~Now, we~~

3.1.2 ~~Which variables explain NEE: feature importance~~

~~We now~~ consider feature importance~~and ALE, which allows~~, ~~allowing~~ us to analyze how the ~~model treats the data sets~~~~models~~
340 ~~rank input variables by their explanatory power~~. For the peak growing season, all nonlinear ML models agree for both stations (Fig. 7, Table A2) that the variables with the most explanatory power are PAR and ~~the diffuse radiation~~~~diffuse PAR~~. Moreover, PAR typically comes first, except for Cubist in the case of Värriö. ~~Overall, during the peak growing season in boreal forests, a daytime CO_2 flux due to photosynthesis prevails over that due to respiration, at least in Hyytiälä (Kolari et al., 2009). Therefore, one can expect that parameters controlling photosynthesis also dominate the NEE response. PAR is theoretically the most~~
345 ~~important variable during the peak growing season to explain photosynthesis (Palmroth and Hari, 2001; Moffat et al., 2010), and the stimulating effect of diffuse radiation on the peak season photosynthesis (diffuse radiation fertilization) is also well-known (Gu et al., 2002). Accordingly, the models consider light-related variables to be the most important. Interestingly, LinRegr chooses diffuse PAR as the most important variable to explain NEE, likely because the dependence of photosynthesis on diffuse PAR can be considered closer to linear.~~

350 The third variable in importance ~~is vapor pressure deficit~~ after PAR and diffuse PAR, as seen by nonlinear models, is VPD (3 cases), air temperature (2 cases), or soil temperature A (1 case). It is good to note that VPD is calculated based on air temperature (see Sec. 2.1), so these variables are not independent. ~~These variables also have a similar effect increasing NEE at high temperatures: due to increasing respiration (driven by temperature increase) and due to dampening photosynthesis (driven by VPD increase). Interestingly, the linear model chooses diffuse radiation as the most important variable to explain NEE, likely~~
355 ~~because the dependence of photosynthesis on diffuse radiation is closest to linear. PAR is theoretically the most important variable during the peak growing season to explain photosynthesis (Palmroth and Hari, 2001). Light response curve, quantifying the dependence of CO₂ flux due to photosynthesis on PAR, saturates at higher PAR values. Respiration does not depend on PAR, but it grows exponentially with temperature. Therefore, PAR, diffuse PAR, and VPD are confirmed as essential drivers of carbon assimilation in numerous studies on photosynthesis in different ecosystems (Gu et al., 2002; Larcher, 2003; Grossiord et al., 2020)~~
360 ~~Particularly for Hyytiälä during the peak growing season, we can expect the relationship of NEE on PAR to be similar to that of photosynthesis, saturating at higher PAR values.~~ growing season, a statistical model showed that daily photosynthesis is most sensitive to light and VPD (Peltoniemi et al., 2015). However, as NEE is the net result of photosynthesis and respiration, and respiration is highly sensitive to temperature, it makes sense that the models pick either VPD or temperature as the third important variable. Ecosystem respiration is the sum of aboveground and belowground respiration, but soil temperature is
365 sometimes considered a better parameter for modelling ecosystem respiration than air temperature (Kolari et al., 2009; Lasslop et al., 2012)

Overall, during the peak growing season in boreal forests, daytime CO₂ flux due to photosynthesis prevails over that due to respiration, at least in Hyytiälä (Kolari et al., 2009). Therefore, one can expect that light control on photosynthesis also dominates the NEE response, and ~~We note that nonlinear ML models typically place several variables close to the third position~~
370 ~~in the feature importance diagram. For Hyytiälä, RF places diffuse fraction close to VPD, followed by air temperature and RH; Cubist and avNNet place intercorrelated soil temperature A and B (R = 0.98, Fig. A1) high. For Värriö, Cubist and avNNet place interdependent VPD, RH, and air temperature in the feature importance diagram within the error bar from each other. Relatively large error bars for these variables suggest that the models seem to have difficulties ranking them, as their order may likely change depending on the data split. At the same time, the models consider light-related variables as the most important~~
375 ~~error bars are smallest for RF, which seems more confident than other nonlinear models in its treatment of interdependent variables. At the same time, the temperature effect is relevant for respiration, and VPD controls stomatal conductance and carbon uptake. Accordingly, the models pick temperature or VPD as~~

Suppose the model chooses one variable before another correlated one. In that case, ~~the third important variable~~ second one can be placed low in the feature importance diagram, as the model, in principle, does not need it anymore. This does not mean,
380 however, that one of the correlated variables explains NEE clearly better than the other: for example, Moffat et al. (2010) showed, using an artificial neural network, that intercorrelated diffuse fraction and diffuse radiation (as well as intercorrelated VPD and RH) have the same explanatory power for the summertime forest NEE, and can be used interchangeably. However, all our models place diffuse PAR higher than diffuse fraction, and they typically place VPD higher than RH.

385 Feature importance for the whole-year setups (Fig. 7) shows another set of most relevant variables lifting soil temperature at the expense of air temperature or VPD (nonlinear models, see Table A2). In many cases, soil temperature becomes the second important variable, sometimes even the first (avNNet, Hyytiälä). The increasing importance of the temperature-related variable is expected because, in the whole-year case, the model needs to capture the seasonality of carbon flux (Mäkelä et al., 2004, 2006), and soil temperature grows in summer and decreases in winter. However, the models' choice of soil temperature over air temperature requires additional explanation. Presumably, the soil temperature is positive during the warm season and nearly constant during winter in the presence of snow. This behavior is in line with NEE, which is also inhibited in winter. Air temperature, in contrast, may display significant variability also in winter. In addition, soil temperature limits plant water use and photosynthesis in spring and autumn (Wu et al., 2012; Lintunen et al., 2020). In the case of the LinRegr, PAR is no longer among the three most important variables, replaced by another soil temperature or diffuse fraction.

3.1.3 How the models use input variables: ALE

395 Proceeding with ALE, we discuss dependencies of NEE on input variables as seen by the models, focusing on the peak growing season so far. ALE demonstrates that NEE decreases with increasing PAR and diffuse radiation for all PAR for all the models (Fig. 8). Nonlinear models capture show the nonlinear dependence of NEE on PAR, which is most pronounced for the RF model. As captured by nonlinear models, NEE response to diffuse radiation is also relatively strong. However, This model shows that NEE saturates at higher PAR values, resembling the light response curve, and for the Värriö data set, NEE levels off at the largest diffuse radiation. High diffuse radiation level, PAR. This could be because high diffuse PAR is observed under a cloudy sky, means and in Värriö that the, the corresponding PAR level can be below already be close to the light saturation point (Ezhova et al., 2018), and therefore NEE increases, inhibiting photosynthesis.

RF and Cubist also capture a nonlinear dependence of NEE on the vapor pressure deficit VPD, which has an optimum value between the low and high values of VPD. At very high VPD, stomatal closure prevents plants from losing water (Running, 1976), affecting again also photosynthesis, also affecting photosynthesis. Besides, high VPD is often associated with high temperature, which increases NEE due to increased respiration. At low VPD, when water vapor pressure at the leaf level and in the atmosphere is about the same, there is no driving force to sustain transpiration. This inhibits water uptake by the roots and generally slows down plant metabolism, also affecting photosynthesis. PAR, diffuse PAR, and VPD are confirmed as essential drivers of carbon assimilation in numerous studies on photosynthesis in different ecosystems (Gu et al., 2002; Larcher, 2003; Grossiord et al., 2020). Particularly for Hyytiälä during the growing season, a statistical model showed that daily photosynthesis is most sensitive to light and VPD (Peltoniemi et al., 2015). Moreover, low VPD is associated with lower PAR and higher diffuse fraction (Fig. A1), pointing at overcast cloudy conditions when photosynthesis is light-limited.

Note that dependencies of NEE on PAR, diffuse radiation PAR, and VPD are qualitatively similar in all studied used nonlinear models, though quantitatively, sensitivity to the corresponding variables somewhat differs. However, the dependence of NEE on air temperature is not the same in all models. In Hyytiälä, RF and Cubist feature an increase of NEE with air temperature, whereas linear model and artificial neural network demonstrate a decreasing dependence LinRegr and avNNet demonstrate a

~~decrease~~. In Värriö, all models except ~~the artificial neural network suggest an increasing~~ avNNet suggest a positive dependence of NEE on air temperature. ~~Increasing~~ The positive dependence is in line with the stomatal control at high temperatures
420 (stomatal closure dampening photosynthesis) and higher soil respiration during the peak growing season.

It is interesting to analyze ALE from different models trained on the input data sets with several temperature variables. Both soil and air temperature are typically included in modeling studies of NEE based on machine learning (Dou and Yang, 2018; Liu et al., 2021; Abbasian et al., 2022). Cai et al. (2020) and Wood (2021) include average, minimum, and maximum air and soil temperature in their studies, adding more interdependent variables in the data sets. Hyytiälä's data set includes air
425 temperature and temperature from A and B soil horizons. In the peak season, all these temperature-related variables show quite similar dynamics. With soil depth, the mean temperature and amplitude of the diurnal temperature cycle decrease, and the time lag between the temperature signals increases. ~~The time delay between air temperature and soil temperature at B horizon is~~
However, horizon B is not too deep and the lag remains generally smaller than half a day. All the models, besides RF, treat ~~Soil~~
soil temperatures A and B as important variables and demonstrate strong but opposite dependencies on these variables (Fig.8).
430 ~~Keeping in mind that~~ As soil temperatures A and B are correlated (Appendix A, Fig. A1), opposite NEE dependencies ~~may~~ must outweigh each other. Strong opposite dependencies on correlated variables should be treated cautiously. ~~The~~ as the models might use them to ~~compensate for the effect on NEE from different temperature variables or for tuning~~ tune towards higher scores on given data sets. In ~~that case~~ the case of correlated soil temperatures, there is no guarantee that this compensation or tuning will work for ~~a~~ even higher temperature, which is currently not represented in the data set. The same conclusion
435 applies to using the model developed for a particular site on the data sets from other sites (Peltoniemi et al., 2015). In contrast, RF shows a strong ~~increasing dependence only on~~ association of NEE only with air temperature and a weak ~~dependence on~~
association with two soil temperature variables.

~~Regarding~~ Now we briefly discuss other variables that have a more minor effect on NEE ~~diffuse~~. Diffuse fraction demonstrates a consistent impact across all models, leading to ~~an~~ some increase in NEE with its rise. This effect likely stems from the
440 ~~significant presence of a diffuse fraction~~ reduction of photosynthesis under an overcast sky, ~~where reduced radiation hampers~~
photosynthesis.

~~In examining the impact of soil temperature A on Net Ecosystem Exchange (NEE), it was observed that, with the exception of the Random Forest (RF) model, an increase in soil temperature is correlated with a rise in NEE at~~ with low radiation and high
diffuse fraction. Note that diffuse fraction and diffuse PAR contain the same information provided PAR is included in the data
445 set. Gross primary production in Hyytiälä and a decline at Värriö. However, within the RF model, a consistent increase in NEE
was noted for both sites. Overall, its overall effect on NEE is minor. An increase in NEE is expected for higher temperatures,
primarily due to the respiration effect has its minimum at the low diffuse PAR and a maximum at the high diffuse PAR compared
to the weak parabolic dependence on diffuse fraction (Ezhova et al., 2018; Neimane-Šroma et al., 2024). That may be why the
models choose diffuse PAR over diffuse fraction. Most models could then deem the diffuse fraction relatively unimportant as
450 they already use diffuse PAR.

~~Relative humidity directly influences Vapor Pressure Deficit (VPD)~~

RH directly influences VPD through a linear relationship ~~-, with VPD adjusting in response to changes in relative humidity levels (eq. (2), Fig. A1).~~ The higher the RH, the closer ambient air is to saturation, and VPD, in this case, is small. Low RH, vice versa, favors higher VPD values. ~~This is captured better by RF and Cubist than by the neural network and linear model.~~ Having VPD as one of the powerful explaining variables should, in principle, diminish the role of RH. ~~However, this is not, as is the case for neural network and linear models. RF and Cubist. However,~~ RH is placed relatively high in the feature importance for ~~these models avNNet and LinRegr,~~ which is also reflected in the significant range of NEE variability due to RH.

In Hyytiälä, all nonlinear models feature an increase in NEE ~~for low with decreasing~~ soil water content. In Värriö, all models feature an increase of NEE with growing-increasing soil water content, and ~~similar behavior is demonstrated by Cubist and neural network~~ in Hyytiälä, Cubist and avNNet demonstrate similar behavior. Note, however, that sensitivity to this variable is quite low for all models, indicating that soil moisture does not limit ecosystem functioning in current conditions. However, this could change in the future, which would perhaps not be captured by the models.

For friction velocity, all models indicate a consistent trend in Hyytiälä, where an increase in friction velocity leads to a decrease in NEE, suggesting that NEE flux is somewhat sensitive to changes in turbulence levels. On the one hand, this could indicate an eddy covariance problem (Moffat et al., 2010). On the other hand, this dependence might reflect physical processes: friction velocity has a weak increasing trend in Hyytiälä due to trees getting taller, which coincides with the weak, increasing trend in carbon uptake but not in respiration (Launiainen et al., 2022). In Värriö, there is no clear dependence between friction velocity and NEE. Generally, this variable holds limited importance in the overall model predictions.

~~Feature importance for the all-season data (Fig. 7) shows another set of most relevant variables bringing up soil temperature at the expense of air temperature or vapor pressure deficit (nonlinear models, see Table A2). In many cases, soil temperature becomes the second important variable, sometimes even the first (neural network, Hyytiälä). The increasing importance of the temperature-related variable is expected because, in the all-season case, the model needs to capture the seasonality of carbon flux (Mäkelä et al., 2004, 2006), and soil temperature grows in summer and decreases in winter. However, the models' choice of soil temperature over air temperature requires additional explanation. Presumably, the soil temperature is positive during the warm season and nearly constant during the snow season. This behavior is in line with NEE, which is also inhibited in winter. Air temperature, in contrast, may display significant variability. In addition, soil temperature limits plant water use and photosynthesis in spring and autumn (Wu et al., 2012; Lintunen et al., 2020). In the case of the linear model, PAR is no longer among the three most important variables, replaced by another soil temperature or the diffuse fraction of radiation., which is to be expected as filtering by friction velocity is applied to the data sets routinely during quality checks.~~

~~The dependence~~ We proceed with the whole-year ALE plots: the dependencies of NEE on light variables (PAR, diffuse radiation) ~~remains PAR remain~~ largely similar to ~~that those~~ for the peak growing season setup (Fig. A3). ~~Nonlinear models~~ Most nonlinear models (except avNNet on Hyytiälä data set) predict that the NEE dependence on air temperature has a minimum in ~~Hyytiälä in~~ the presence of negative temperatures in the data set, suggesting larger NEE during the cold season and ~~periods with the warmest soil. NEE has similar dynamics for soil temperature~~ At the warmest summer periods. This might reflect the absence of GPP-photosynthesis in the cold season and the ~~increase of respiration for high~~ increased respiration accompanied by inhibited photosynthesis for the highest temperatures. In ~~Värriö, NEE dependencies on air temperature also~~

generally have minima. Dependence on soil temperature A is decreasing. Hyytiälä, NEE dependence on soil temperature A also has a minimum. In Värriö, NEE decreases with increasing soil temperature until it plateaus at around 15°C in the case of RF and avNNet. Note that for Hyytiälä, NEE dependencies on soil temperatures B and A are again of opposite sign for all models besides except RF. The linear model LinRegr fails on the Hyytiälä data set, showing a weak association of NEE with air temperature but featuring lower NEE and stronger carbon sink at low, even negative soil temperatures. The failure of the linear model on the whole season cycle LinRegr on the whole year data could be related due to its inability to capture essentially nonlinear air temperature dependence the nonlinear dependence of NEE on temperature, which becomes important on the all-season significant on a whole-season scale.

495 Considering less critical variables, the dependencies remain mainly the same. In some cases, however, the neural network avNNet demonstrates dependencies inconsistent with expected behavior, i.e.e.g., featuring a strong carbon sink at high air temperature in Hyytiälä or stronger carbon sink under low RH conditions. It is worth mentioning that the dependence on soil water content has become is quite complicated in Hyytiälä, with a minimum and a maximum. This could be related to data containing subsets with high water content at low temperatures when photosynthesis is inhibited, e.g., during snowmelt or late autumn. In any case, as for the peak growing season setup, the sensitivity of NEE to this variable is low.

500 Finally, if the most important input variables for these the studied sites are the same and the dependencies of NEE on these variables are similar as in the case of RF and, to a lesser extent, Cubist, one could expect that it is possible to build a more generic model, which would be able to give reasonable results for many different boreal forest sites. We, therefore, built one model based on all the data in the following section.

505 3.2 NEE modelling: mixed data set

In this section, we report the results of NEE modeling using all three available data sets, which consist of Set 2 (Table 3), which consists of mixed data from pre-thinning Hyytiälä (referred to just as Hyytiälä), Värriö and post-thinning Hyytiälä. We aimed to understand how the models perform in the following cases: 1) mixed data set, containing data from both sites including post-thinning Hyytiälä, without any separation or benchmarking the data (setups Peak Without Site and All Without Site, Table 3); 2) mixed data set, but we introduce three binary dummy variables that identify the site (setups Peak With Site and All With Site, Table 3). Three binary variables were used instead of a single categorical one due to some models requiring real numbers as input (Hancock and Khoshgoftaar, 2020).

3.2.1 Assessing model performance on a mixed data set using accuracy metrics

515 The determination coefficients for mixed data sets are shown in Fig.9, separately for the model runs with and without the variables for the site identity. Adding site variables to the data set slightly improves the correlation coefficient R^2 (within 3.5%), which remains high for the best models, RF and Cubist (0.84-0.87 for the peak season, 0.86-0.89 for the whole season). The results are marginally worse for the peak growing season. Comparing this result to the results for the separate stations (Fig. 1), we note that the scores are closer to those for Hyytiälä. This is likely could be because Hyytiälä data prevails in the compiled data set. Interestingly, the linear model However, a trial run with equal inputs from different sets (Hyytiälä pre-thinned

520 + Hyytiälä post-thinned + Värriö) shows that R^2 was only marginally lower, by 0.02 for the nonlinear ML models (Figs. A5, A6). This finding suggests that factors other than the prevalence of the Hyytiälä data set may be important: for example, the value range of the data. Hyytiälä data set has a larger NEE value range compared to Värriö, and that could be the reason for better Hyytiälä R^2 -coefficient, as mentioned in sec. 3.1.1. Therefore, one could expect larger R^2 -coefficients for any mixed sets containing a sufficient amount of Hyytiälä data when compared to the Värriö data set. Interestingly, LinRegr performs worse than others-other models on a compiled data set, even during-for the peak growing season. The scores-for-linear-models-are also-significantly-lower-than-LinRegr R^2 -coefficient on the mixed data set is clearly lower than on the Hyytiälä scores data set (drop from 0.85 to 0.80 for the peak growing season and from 0.76 to 0.68 for the whole year).

As said, site variables do not have a significant effect on R^2 -coefficients, but the advantage is more evident for RMSE (Fig. 10). In-general, RMSE for the peak growing season data is generally larger than for the whole season. This-is, likely because the fluctuations and errors of NEE measurements outside the growing season are relatively small. In addition, the flux random error increases with the flux magnitude within the growing season. If we compare the models for-the-peak-growing-season with and without site variables, we see that adding site variables reduces RMSE by 10-13%: from about 2.4 to 2.15 $\mu\text{mol s}^{-1} \text{m}^{-2}$ in-the-case-of-best-performing-models. For-all-season-data-sets, the-reduction-of-RMSE-is-for-the-peak-growing-season-and from about 1.8 to 1.6 $\mu\text{mol s}^{-1} \text{m}^{-2}$ for the whole year. Considering models for-the-trained-on-data-of separate sites, there-is-a-slight reduction-in-RMSE-score-in-the-model, including-site-variables-and-all-season-RMSE scores in the models with site variables are somewhat smaller compared to the models trained on the Hyytiälä data set, compared-to-probably due to the presence of Värriö data with smaller RMSE than Hyytiälä data (Fig. 2) or due to the larger size of the mixed data set. Overall, introducing the site variables barely-improve-in-the-mixed-data-set barely-improves the correlation between measured and modeled points but reduce-reduces the scatter in the plot presenting measured vs modeled points.

540 3.2.2 ALE and feature Feature importance for the mixed data set

It-is-interesting-to-assess-the-position-of-the-site-variable-in-the-We assess the feature importance diagrams provided by the models on the mixed data sets, paying special attention to the ranking of the site variables (Fig. 11). Consider-first-the-peak growing season. Note that the vapor pressure deficit is no longer within the three most important variables for the RF model and, Table A2). It follows quite clearly from Table A2 that the models' choice of the most important input parameters becomes more aligned when they are trained on the mixed data set. It-is-replaced-by-the-soil-water-content-for-the-setup-without-site variables-and-by-the-For example, all the models, without exception, choose PAR as the most important variable in both peak-season and whole-year setups. During the peak season, the second variable in the feature importance diagrams is diffuse PAR (6 setups out of 8) or VPD (2 out of 8). Continuing with the peak season, site parameter 'Värriö' site-variable-for-the model-with-site-variables. Värriö-is-located-at-higher-latitudes-and-appears only as the third variable in the corresponding setups (replaced in some models with VPD or diffuse PAR). In the setup without site parameters, the third important variable is VPD or diffuse PAR or soil water content in case of RF. The latter observation is interesting as Värriö has different soil characteristics: soil moisture is lower there (Fig. A2). This-input-variable-could-then-be-considered-, and RF might have used it

as a replacement of the site variable by the RF model. However, other nonlinear models consider VPD the third most important variable when no

555 For the whole-year setups, the second variable after PAR in the feature importance diagrams is almost always soil temperature A (7 out of 8 cases) or diffuse PAR (1 out of 8 cases). (Recall that the Hyytiälä feature importance set contained Soil temperature B, not A. Replacement of this variable by the temperature at A horizon is because Soil temperature B is not in the data set anymore as it was not measured in Värriö). The third variable is diffuse PAR (5 out of 8 cases) or VPD/soil temperature/air temperature (one case each). Note that site variables are introduced. Cubist treats not among the three most important in
560 the whole-season setups. Instead, the models retain NEE dependence on soil temperature, which allows them to reproduce a seasonal cycle and choose over the site variables diffuse PAR, VPD or air temperature. Nevertheless, site variables appear among the six highest input variables in the feature importance diagrams, and as follows from Fig.10, they help to reduce the RMSE.

Another observation is that among site variables, the models put 'Värriö' and VPD as the third-fourth important variables
565 when the site variables are included. The neural network still considers VPD a more powerful NEE explanation variable than any site variables' highest in the peak-season setups but 'Hyytiälä' in the whole-year setups. However, as mentioned before, it should be possible for the models to use them interchangeably.

3.2.3 ALE for the mixed data set

Judging by ALE (Fig. 12) Figs. 12, the models prescribe higher values of NEE to the drier cases, which is in line with how
570 the ecosystem functions under drier conditions (reduction of photosynthesis). When site variables are added, RF and Cubist choose site variable A4), dependencies of NEE on light variables (PAR and diffuse PAR) for all setups in Set 2 are similar to those for separate stations (Figs. A3, A3). In the peak season, the nonlinear models suggest that the third important variable is 'Värriö' as the third important. From ALE, one could see for the setups with site parameters. From Fig. 12, it can be seen that the modeled NEE increases if 'Värriö' changes from zero to one. The models then use this site variable to make all NEE
575 values at Värriö somewhat higher than the general mean value for all three sites, which is the case due to lower tree biomass. Interestingly, the linear model does not use the site variable 'Värriö' at all (its value is zero). Similarly, models use the variable 'Hyytiälä' when it is equal to one to decrease NEE, and this decrease is less pronounced for the best-performing Cubist and RF than for the other models. Finally, when 'HyytiäläT' variable is equal to one, RF and Cubist slightly increase NEE, whereas the other models decrease NEE. Because the prevailing data set is still Hyytiälä pre-thinned, this data set likely dictates the
580 base values chosen by the models. Therefore, a moderate increase of NEE for the Hyytiälä thinned data set and a stronger NEE increase for the Värriö station is reasonable. Interestingly, LinRegr does not use the site variable 'Värriö' at all.

Furthermore, for the setup with site variables to predict NEE in peak growing season, all the models display increasing
dependence on air temperature, following theoretical expectations due to increasing respiration and reduced photosynthesis. However, NEE dependencies on soil temperature A somewhat decrease for all the models except RF. Note that neural network
585 and linear models still have much stronger NEE dependencies on VPD than RF and Cubist. Similar to setups for separate stations, In the peak-season setup without site variables, soil water content is one of the relevant variables chosen by the

~~models, especially RF. Judging by ALE (Fig. 12), the models likely use relative humidity to compensate for a too-strong effect of VPD.~~

590 ~~Modeling the all-season data sets~~ models prescribe higher values of NEE to the drier cases, which is in line with how the ecosystem functions under drier conditions (reduction of photosynthesis). Similarly, for the whole-season setup without site variables, we note that NEE ~~still has the same decreasing dependence on~~ decreases strongly with increasing soil water content (Fig. A4), ~~and the dependence is quite strong,~~ in contrast to what was observed when we modeled separate sites. However, the feature importance order for the RF and Cubist models repeats that for single site Värriö: PAR, soil temperature A, and diffuse radiation (Fig. 11). (Recall that the Hyytiälä feature importance set contained Soil temperature B, not A. Replacement of this variable by the temperature at A horizon is because Soil temperature B is not in the data set anymore as it was not measured in Värriö). The neural network, similar to the model results ALE plots for both the peak-season and whole-season setups (Figs. 12, A4) demonstrate clearly how soil water content loses its strong position when site variables are introduced and how the NEE dependence on this variable again becomes complex, in line with what is observed for separate stations.

600 ~~NEE dependencies on VPD are qualitatively similar for mixed data sets in those for separate sites, has a strong accent~~ . LinRegr and avNNet still have strong and opposite NEE dependencies on VPD and air temperature independently of the presence of the site variables in the input RH, similar to their performance on the Hyytiälä data set. Note that site variables are not among the three most important in the all-season case. Instead, the models retain their dependence on soil temperature, which allows them to reproduce a seasonal cycle. This can be interpreted as the sign that on the all-season scale, the model deems the changes in NEE due to the seasonal cycle more critical than those associated with the site-to-site change. 605 Nevertheless, site variables appear among the six most important features in the feature importance diagrams, and as follows from Fig. 10, they help to reduce the RMSE. These models might use variable RH to compensate for a too-strong modelled effect of VPD on NEE.

Further looking at the all-season setup, dependencies of NEE on PAR, diffuse radiation, and ~~Interestingly, all models display~~ a positive dependence of NEE on air temperature for the peak growing season and setup with site variables, unlike avNNet and LinRegr on Hyytiälä data. Positive dependence is in line with theoretical expectations due to increasing respiration and reduced photosynthesis with increasing temperature within the peak season. At the same time, NEE somewhat decreases with increasing soil temperature A for all models (Fig. A4) are similar to those for separate stations (Fig. A3). RF demonstrates a somewhat stronger increasing NEE at higher temperatures than other models. All the models use the 'Hyytiälä' site variable to slightly decrease NEE, and the ~~the models except RF;~~ however, this effect of soil temperature on NEE, as captured by the models, is much weaker than that of air temperature. 615

On the whole year scale, all nonlinear models demonstrate rather similar NEE dependencies on different variables (except strong NEE dependencies on VPD and RH partially outweighing each other as modelled by avNNet), which was also the case for the separate Värriö ² variable to increase NEE, with the exception of the linear model, which does not use the ² setup. This could be due the data from Värriö ² variable at all.

620 From both ALE plots for the peak season and all-season setups (Figs. 12, A4), it follows clearly how soil water content loses its strong position when site variables are introduced and how the NEE dependence on this variable again becomes complex,

~~in line with what is observed for separate stations~~ that has a long dormant season: one of the main tasks of the models is to reproduce seasonal cycle, for which the nonlinear models use soil temperature in a similar manner.

625 Generally, RF performed more in line with theoretical expectations ~~from ecophysiological research~~ than other models ~~on the input when trained on the~~ data set containing interdependent variables, ~~such as VPD depending on air temperature and humidity or several temperature variables. The linear model and the Neural network.~~ LinRegr and the avNNet demonstrate strong dependencies of NEE on VPD, which they likely compensate for by relatively strong dependencies ~~of NEE~~ on air temperature and ~~relative humidity. In some cases, these dependencies contradict the expectations based on ecosystem functioning RH.~~ Due to that, some ALE may appear counterintuitive (e.g., strengthening of carbon sink with increasing air temperature ~~for~~ 630 ~~Hyytiälä during during the~~ peak season), ~~contradicting the expectations based on general knowledge of ecosystem functioning.~~ In addition, all models except RF demonstrate strong opposite associations with soil temperature A and B when both variables are available (Fig. 8).

4 Conclusions

We modeled NEE at two sites in boreal forest ~~separately~~: one in central Finland and one in the Finnish subarctic. We focused 635 on the peak growing season and ~~all-season data set~~ whole-year data sets. Peak growing season NEE for separate sites can be modeled reasonably well even with ~~the linear a simple linear regression~~ model. However, ~~the linear model~~ Linear Regression performs significantly worse than nonlinear ML models in the case of ~~several sites and all-season~~ the mixed data sets from both sites or whole-year data sets.

The most powerful explaining variables in the peak growing season ~~setup setups~~ are PAR, diffuse PAR, and vapor pressure 640 deficit (or air temperature); in the case of the ~~all-season setup~~ whole-year setups, such variables are PAR, ~~diffuse PAR, and soil temperature~~ soil temperature and diffuse PAR. This is a robust result reproduced by most of the models used in this study. High vapor pressure deficit dampens photosynthesis and, hence, makes NEE increase. This effect is essential during the peak growing season. The models presumably used soil temperature to account for the change in NEE within a seasonal cycle. ~~Based on ALE, the models that give qualitative dependencies on different variables in line with theoretical expectations are mainly~~ 645 ~~Random Forest and Cubist. This result aligns with many studies that used RF based on its best performance compared with other models. At the same time, in setups with several interdependent variables, the Linear model and artificial Neural network often display strong opposite dependencies on the interdependent variables, largely canceling their total effect on NEE.~~

To build a joint model for several sites, we added site variables. The model is more sensitive to these variables within the peak growing season, whereas soil temperature retains its importance for the ~~all-season~~ whole-year data sets. In the ~~mixed data~~ 650 ~~setup, the model scores seem to be governed by the most represented set, which in our case was Hyytiälä pre-thinned. In the absence of site variables, the models replace it with~~ absence of site-specific variables, Random Forest ranks soil water content, the variable that differs most between the sites: ~~in our case, it is soil water content, as the third most important in the feature~~ importance diagram. NEE dependence on soil water content and the importance of this variable for NEE predictions change drastically for the models built on the data sets, including and excluding site variables.

655 Our ALE results suggest that ~~RF and Cubist show~~ Cubist and especially Random Forest display more robust behavior modeling complex nonlinear dependence of net ecosystem exchange on the set of interconnected variables. They could qualitatively reproduce the theoretically expected dependencies of NEE on the major climatic drivers of ecosystem processes under different conditions and for several sites. ~~At the same time, the Linear model and Neural network tend to overweigh some variables and compensate for those with the help of~~ This result aligns with many studies that used Random Forest based on its best performance compared with other models. Additionally, Linear Regression and Model Averaged Neural Networks tend to overemphasize certain variables while compensating with other interdependent variables. In our modeling study, ~~the variables used by the Linear model and Neural network for compensation included~~ Linear Regression and Model Averaged Neural Networks compensated using variables like air temperature and relative humidity, which are ~~very~~ highly sensitive to changing climate conditions.

665 All in all, it should be noted that the models' performance changes depending on a given setup, so no single recommendation suggesting or prohibiting a specific model can be given. This is, instead, a case-by-case issue. Therefore, we call for broader usage of Explainable Artificial Intelligence methods when applying ML methods, especially when choosing the most suitable model. Feature importance and ALE plots together allow for a direct comparison between ML model functioning and process-based models.

670 Finally, we showed that even a simple way to account for the difference between the sites decreases RMSE and improves the model. The next step is to introduce a more suitable variable, allowing us to distinguish the ecosystems from each other. As Hyytiälä data are split into pre-thinned and post-thinned, we need a variable that could account for this change in the vegetation. The best candidates for this could be satellite-based NDVI and LAI (Launiainen et al., 2022; Zhu et al., 2023), which we plan to add to our data set instead of site variables.

675 *Code availability.* TEXT

Data availability. TEXT

Code and data availability. TEXT

Sample availability. TEXT

Video supplement. TEXT

680 *Author contributions.* EE, AL, KH and MK designed and conceptualized the study. TL performed modeling and prepared figures, wrote the manuscript (Introduction and Section 2). EE interpreted results and wrote the manuscript (Introduction, Section 3 and Conclusion). AL, PK, IM, KH and MK contributed with results interpretation, review and editing. All the authors commented on the manuscript.

Competing interests. The authors declare that they have no conflict of interest.

Acknowledgements. We acknowledge the following projects: ACCC Flagship funded by the Academy of Finland grant number 337549 (UH) and 337552 (FMI), Academy professorship funded by the Academy of Finland (grant no. 302958), Academy of Finland projects no. 1325656, 311932, 334792, 316114, 325647, 325681, 347782, “Quantifying carbon sink, CarbonSink+ and their interaction with air quality” INAR project funded by Jane and Aatos Erkko Foundation, and HORIZON EUROPE (Project 101056921 — GreenFeedBack). University of Helsinki support via ACTRIS-HY is acknowledged. University of Helsinki Doctoral Programme in Atmospheric Sciences is acknowledged. Support of the technical and scientific staff in Hyytiälä is gratefully acknowledged.

690 References

- Aalto, J., Anttila, V., Kolari, P., Korpela, I., Isotalo, A., Levula, J., Schiestl-Aalto, P., and Bäck, J.: Hyytiälä SMEAR II forest year 2020 thinning tree and carbon inventory data, <https://doi.org/10.5281/zenodo.7639833>, 2023.
- Abbasian, H., Solgi, E., Hosseini, S. M., and Kia, S. H.: Modeling terrestrial net ecosystem exchange using machine learning techniques based on flux tower measurements, *Ecological Modelling*, 466, 109 901, 2022.
- 695 Artaxo, P., Hansson, H.-C., Andreae, M. O., Bäck, J., Alves, E. G., Barbosa, H. M. J., Bender, F., Bourtsoukidis, E., Carbone, S., Chi, J., Decesari, S., Després, V. R., Ditas, F., Ezhova, E., Fuzzi, S., Hasselquist, N. J., Heintzenberg, J., Holanda, B. A., Guenther, A., Hakola, H., Heikkinen, L., Kerminen, V.-M., Kontkanen, J., Krejci, R., Kulmala, M., Lavric, J. V., De Leeuw, G., Lehtipalo, K., Machado, L. A. T., McFiggans, G., Franco, M. A. M., Meller, B. B., Morais, F. G., Mohr, C., Morgan, W., Nilsson, M. B., Peichl, M., Petäjä, T., Praß, M., Pöhlker, C., Pöhlker, M. L., Pöschl, U., Von Randow, C., Riipinen, I., Rinne, J., Rizzo, L. V., Rosenfeld, D., Silva Dias, M.
- 700 A. F., Sogacheva, L., Stier, P., Swietlicki, E., Sörgel, M., Tunved, P., Virkkula, A., Wang, J., Weber, B., Yáñez-Serrano, A. M., Zieger, P., Mikhailov, E., Smith, J. N., and Kesselmeier, J.: Tropical and boreal forest – atmosphere interactions: A review, *Tellus B Chem. Phys. Meteorol.*, 74, 24, 2022.
- Aubinet, M., Vesala, T., and Papale, D.: *Eddy covariance: a practical guide to measurement and data analysis*, Springer Science & Business Media, 2012.
- 705 Berrar, D.: Cross-Validation, in: *Encyclopedia of Bioinformatics and Computational Biology*, edited by Ranganathan, S., Gribskov, M., Nakai, K., and Schönbach, C., pp. 542–545, Academic Press, Oxford, <https://doi.org/https://doi.org/10.1016/B978-0-12-809633-8.20349-X>, 2019.
- Breiman, L.: Random Forests, *Machine Learning*, 45, 5–32, <https://doi.org/10.1023/A:1010933404324>, 2001.
- Cai, J., Xu, K., Zhu, Y., Hu, F., and Li, L.: Prediction and analysis of net ecosystem carbon exchange based on gradient boosting regression and random forest, *Applied energy*, 262, 114 566, 2020.
- 710 Dou, X. and Yang, Y.: Estimating forest carbon fluxes using four different data-driven techniques based on long-term eddy covariance measurements: Model comparison and evaluation, *Science of the Total Environment*, 627, 78–94, 2018.
- Dwivedi, R., Dave, D., Naik, H., Singhal, S., Omer, R., Patel, P., Qian, B., Wen, Z., Shah, T., Morgan, G., et al.: Explainable AI (XAI): Core ideas, techniques, and solutions, *ACM Computing Surveys*, 55, 1–33, 2023.
- 715 Ezhova, E., Ylivinkka, I., Kuusk, J., Komsaare, K., Vana, M., Krasnova, A., Noe, S., Arshinov, M., Belan, B., Park, S.-B., Lavric, J. V., Heimann, M., Petaja, T., Vesala, T., Mammarella, I., Kolari, P., Bäck, J., Rannik, U., Kerminen, V.-M., and Kulmala, M.: Direct effect of aerosols on solar radiation and gross primary production in boreal and hemiboreal forests, *Atmospheric Chemistry and Physics*, 18, 17 863–17 881, 2018.
- Fernández-Delgado, M., Sirsat, M. S., Cernadas, E., Alawadi, S., Barro, S., and Febrero-Bande, M.: An extensive experimental survey of regression methods, *Neural Networks*, 111, 11–34, 2019.
- 720 Grossiord, C., Buckley, T. N., Cernusak, L. A., Novick, K. A., Poulter, B., Siegwolf, R. T. W., Sperry, J. S., and McDowell, N. G.: Plant responses to rising vapor pressure deficit, *New Phytologist*, 226, 1550–1566, <https://doi.org/https://doi.org/10.1111/nph.16485>, 2020.
- Gu, L., Baldocchi, D., Verma, S. B., Black, T., Vesala, T., Falge, E. M., and Dowty, P. R.: Advantages of diffuse radiation for terrestrial ecosystem productivity, *Journal of Geophysical Research: Atmospheres*, 107, ACL–2, 2002.
- 725 Hancock, J. T. and Khoshgoftaar, T. M.: Survey on categorical data for neural networks, *J. Big Data*, 7, 28, <https://doi.org/10.1186/S40537-020-00305-W>, 2020.

- Hari, P. and Kulmala, M.: Station for Measuring Ecosystem-Atmosphere Relations (SMEAR II), *Boreal Environment Research*, 10, 315–322, 2005.
- Hari, P., Kulmala, M., Pohja, T., Lahti, T., Siivola, E., Palva, L., Aalto, P., Hämeri, K., Vesala, T., Luoma, S., and Pulliainen, E.:
730 Air pollution in eastern Lapland : challenge for an environmental measurement station, *Silva Fennica* 1994. 28(1): 29–39., 28,
<https://doi.org/10.14214/sf.a9160>, 1994.
- Hastie, T., Tibshirani, R., Friedman, J. H., and Friedman, J. H.: *The elements of statistical learning: data mining, inference, and prediction*, vol. 2, Springer, 2009.
- Jung, Y.: Multiple predicting K-fold cross-validation for model selection, *Journal of Nonparametric Statistics*, 30, 197–215, 2018.
- 735 Junttila, V., Minunno, F., Peltoniemi, M., Forsius, M., Akujärvi, A., Ojanen, P., and Mäkelä, A.: Quantification of forest carbon flux
and stock uncertainties under climate change and their use in regionally explicit decision making: Case study in Finland, *Ambio*,
<https://doi.org/10.1007/s13280-023-01906-4>, 2023.
- Kämäräinen, M., Lintunen, A., Kulmala, M., Tuovinen, J.-P., Mammarella, I., Aalto¹, J., Vekuri, H., and Lohila, A.: Evaluation of gradient
boosting and random forest methods to model subdaily variability of the atmosphere–forest CO₂ exchange, *Biogeosciences Discussions*,
740 2022, 1–24, 2023.
- Kolari, P., Kulmala, L., Pumpanen, J., Launiainen, S., Ilvesniemi, H., Hari, P., and Nikinmaa, E.: CO₂ exchange and component CO₂ fluxes
of a boreal Scots pine forest, *Boreal Environment Research*, 14, 761–783, 2009.
- Kuhn, M.: Building predictive models in R using the caret package, *Journal of Statistical Software*, 28, 1–26, 2008.
- Kuhn, M.: caret: Classification and Regression Training, <https://cran.r-project.org/web/packages/caret/index.html>, r package version 6.0-90,
745 2023.
- Kuhn, M. and Johnson, K.: *Applied Predictive Modeling*, Springer, 2013.
- Kulmala, M., Ezhova, E., Kalliokoski, T., Noe, S., Vesala, T., Lohila, A., Liski, J., Makkonen, R., Bäck, J., Petäjä, T., and Kerminen, V.-M.:
CarbonSink+: Accounting for multiple climate feedbacks from forests, *Boreal Environment Research*, 25, 145–159, 2020.
- Kulmala, M., Cai, R., Ezhova, E., Deng, C., Stolzenburg, D., Dada, L., Guo, Y., Yan, C., Peräkylä, O., Lintunen, A., Nieminen, T., Kokko-
750 nen, T., Sarnela, N., Petäjä, T., and Kerminen, V.-M.: Direct link between the characteristics of atmospheric new particle formation and
Continental Biosphere-Atmosphere-Cloud-Climate (COBACC) feedback loop, *Boreal Environment Research*, 28, 1, 2023.
- Kutner, M. H., Nachtsheim, C. J., Neter, J., and Li, W.: *Applied Linear Statistical Models*, McGraw-Hill, New York, 5th edn., 2004.
- Larcher, W.: *Physiological plant ecology: ecophysiology and stress physiology of functional groups*, Springer Science & Business Media,
2003.
- 755 Lasslop, G., Migliavacca, M., Bohrer, G., Reichstein, M., Bahn, M., Ibrom, A., Jacobs, C., Kolari, P., Papale, D., Vesala, T., et al.: On the
choice of the driving temperature for eddy-covariance carbon dioxide flux partitioning, *Biogeosciences*, 9, 5243–5259, 2012.
- Launiainen, S., Katul, G. G., Leppä, K., Kolari, P., Aslan, T., Grönholm, T., Korhonen, L., Mammarella, I., and Vesala, T.: Does
growing atmospheric CO₂ explain increasing carbon sink in a boreal coniferous forest?, *Global Change Biology*, 28, 2910–2929,
<https://doi.org/https://doi.org/10.1111/gcb.16117>, 2022.
- 760 Liaw, A. and Wiener, M.: Classification and Regression by randomForest, *R News*, 2, 18–22, <https://CRAN.R-project.org/doc/Rnews/>, 2002.
- Lintunen, A., Paljakka, T., Salmon, Y., Dewar, R., Riikonen, A., and Hölttä, T.: The influence of soil temperature and water content on
belowground hydraulic conductance and leaf gas exchange in mature trees of three boreal species, *Plant, Cell & Environment*, 43, 532–
547, 2020.

- Liu, J., Zuo, Y., Wang, N., Yuan, F., Zhu, X., Zhang, L., Zhang, J., Sun, Y., Guo, Z., Guo, Y., et al.: Comparative analysis of two machine learning algorithms in predicting site-level net ecosystem exchange in major biomes, *Remote Sensing*, 13, 2242, 2021.
- Mäkelä, J., Knauer, J., Aurela, M., Black, A., Heimann, M., Kobayashi, H., Lohila, A., Mammarella, I., Margolis, H., Markkanen, T., Susiluoto, J., Thum, T., Viskari, T., Zaehle, Z., and Aalto, T.: Parameter calibration and stomatal conductance formulation comparison for boreal forests with adaptive population importance sampler in the land surface model JSBACH, *Geoscientific Model Development*, 12, 4075–4098, 2019.
- Mammarella, I., Peltola, O., Nordbo, A., Järvi, L., and Rannik, Ü.: Quantifying the uncertainty of eddy covariance fluxes due to the use of different software packages and combinations of processing steps in two contrasting ecosystems, *Atmospheric Measurement Techniques*, 9, 4915–4933, 2016.
- Moffat, A. M., Beckstein, C., Churkina, G., Mund, M., and Heimann, M.: Characterization of ecosystem responses to climatic controls using artificial neural networks, *Global Change Biology*, 16, 2737–2749, 2010.
- Molnar, C.: Interpretable machine learning, Lulu. com, 2020.
- Molnar, C., Casalicchio, G., and Bischl, B.: iml: An R package for interpretable machine learning, *Journal of Open Source Software*, 3, 786, 2018.
- Monteith, J. and Unsworth, M.: Principles of environmental physics: plants, animals, and the atmosphere, Academic Press, 2013.
- Mäkelä, A., Hari, P., Berninger, F., Hänninen, H., and Nikinmaa, E.: Acclimation of photosynthetic capacity in Scots pine to the annual cycle of temperature, *Tree Physiology*, 24, 369–376, 2004.
- Mäkelä, A., Kolari, P., Karimäki, J., Nikinmaa, E., Perämäki, M., and Hari, P.: Modelling five years of weather-driven variation of GPP in a boreal forest, *Agricultural and Forest Meteorology*, 139, 382–398, 2006.
- Neimane-Šroma, S., Durand, M., Lintunen, A., Aalto, J., and Robson, T. M.: Shedding light on the increased carbon uptake by a boreal forest under diffuse solar radiation across multiple scales, *Global Change Biology*, 30, e17 275, <https://doi.org/https://doi.org/10.1111/gcb.17275>, e17275 GCB-23-3034.R2, 2024.
- Palmroth, S. and Hari, P.: Evaluation of the importance of acclimation of needle structure, photosynthesis, and respiration to available photosynthetically active radiation in a Scots pine canopy, *Canadian Journal of Forest Research*, 31, 1235–1243, 2001.
- Peltoniemi, M., Pulkkinen, M., Aurela, M., Pumpanen, J., Kolari, P., and Mäkelä, A.: A semi-empirical model of boreal-forest gross primary production, evapotranspiration, and soil water — calibration and sensitivity analysis, *Boreal Environment Research*, 20, 151–171, 2015.
- Petäjä, T., Tabakova, K., Manninen, A., Ezhova, E., O'Connor, E., Moisseev, D., Sinclair, V. A., Backman, J., Levula, J., Luoma, K., Virkkula, A., Paramonov, M., Rätty, M., Äijälä, M., Heikkinen, L., Ehn, M., Sipilä, M., Yli-Juuti, T., Virtanen, A., Ritsche, M., Hickmon, N., Pulik, G., Rosenfeld, D., Worsnop, D., Bäck, J., Kulmala, M., and Kerminen, V.-M.: Influence of biogenic emissions from boreal forests on aerosol–cloud interactions, *Nature Geoscience*, 15, 42–47, 2022.
- Quinlan, J. R.: Cubist: Rule- and Instance-Based Regression Modeling, <https://CRAN.R-project.org/package=cubist>, R package version 0.4.2.1, 1992.
- Reitz, O., Graf, A., Schmidt, M., Ketzler, G., and Leuchner, M.: Upscaling net ecosystem exchange over heterogeneous landscapes with machine learning, *Journal of Geophysical Research: Biogeosciences*, 126, e2020JG005 814, 2021.
- Ripley, B. D.: Pattern recognition and neural networks, Cambridge university press, 2007.
- Ross, J. and Sulev, M.: Sources of errors in measurements of PAR, *Agricultural and Forest Meteorology*, 100, 103–125, 2000.
- Running, S. W.: Environmental control of leaf water conductance in conifers, *Canadian Journal of Forest Research*, 6, 104–112, 1976.

- Shirley, I. A., Mekonnen, Z. A., Grant, R. F., Dafflon, B., and Riley, W. J.: Machine learning models inaccurately predict current and future high-latitude C balances, *Environmental Research Letters*, 18, 014 026, 2023.
- 805 Tagesson, T., Schurgers, G., Horion, S., Ciais, P., Tian, F., Brandt, M., Ahlström, A., Wigneron, J.-P., Ardö, J., Olin, S., Fan, L., Wu, Z., and Fensholt, R.: Recent divergence in the contributions of tropical and boreal forests to the terrestrial carbon sink, *Nature Ecology & Evolution*, 4, 202–209, 2020.
- Tang, J., Zhou, P., Miller, P. A., Schurgers, G., Gustafson, A., Makkonen, R., Fu, Y. H., and Rinnan, R.: High-latitude vegetation changes will determine future plant volatile impacts on atmospheric organic aerosols, *npj Climate and Atmospheric Science*, 6, 147, 2023.
- Wood, D. A.: Net ecosystem carbon exchange prediction and insightful data mining with an optimized data-matching algorithm, *Ecological Indicators*, 124, 107 426, 2021.
- 810 Wu, S. H., Jansson, P.-E., and Kolari, P.: The role of air and soil temperature in the seasonality of photosynthesis and transpiration in a boreal Scots pine ecosystem, *Agricultural and Forest Meteorology*, 156, 85–103, 2012.
- Zeng, J., Matsunaga, T., Tan, Z.-H., Saigusa, N., Shirai, T., Tang, Y., Peng, S., and Fukuda, Y.: Global terrestrial carbon fluxes of 1999–2019 estimated by upscaling eddy covariance data with a random forest, *Scientific data*, 7, 313, 2020.
- Zhang, A., Lipton, Z. C., Li, M., and Smola, A. J.: *Dive into deep learning*, Cambridge University Press, 2023.
- 815 Zhou, J., Li, E., Wei, H., Li, C., Qiao, Q., and Armaghani, D. J.: Random forests and cubist algorithms for predicting shear strengths of rockfill materials, *Applied sciences*, 9, 1621, 2019.
- Zhu, X.-J., Yu, G.-R., Chen, Z., Zhang, W.-K., Han, L., Wang, K.-F., Chen, S.-P., Liu, S.-M., Wang, H.-M., Yan, J.-H., Tan, J.-L., Zhang, F.-W., Zhao, F.-H., Li, Y.-N., Zhang, Y.-P., Shi, P.-L., Zhu, J.-J., Wu, J.-B., Zhao, Z.-H., Hao, Y.-B., Sha, L.-Q., Zhang, Y.-C., Jiang, S.-C., Gu, F.-X., Wu, Z.-X., Zhang, Y.-J., Zhou, L., Tang, Y.-K., Jia, B.-R., Li, Y.-K., Song, Q.-H., Dong, G., Gao, Y.-H., Jiang, Z.-D., Sun, 820 D., Wang, J.-L., He, Q.-H., Li, X.-H., Wang, F., Wei, W.-X., Deng, Z.-M., Hao, X.-X., Li, Y., Liu, X.-L., Zhang, X.-F., and Zhu, Z.-L.: Mapping Chinese annual gross primary productivity with eddy covariance measurements and machine learning, *Science of The Total Environment*, 857, 159 390, <https://doi.org/https://doi.org/10.1016/j.scitotenv.2022.159390>, 2023.

R² Coefficient Scores

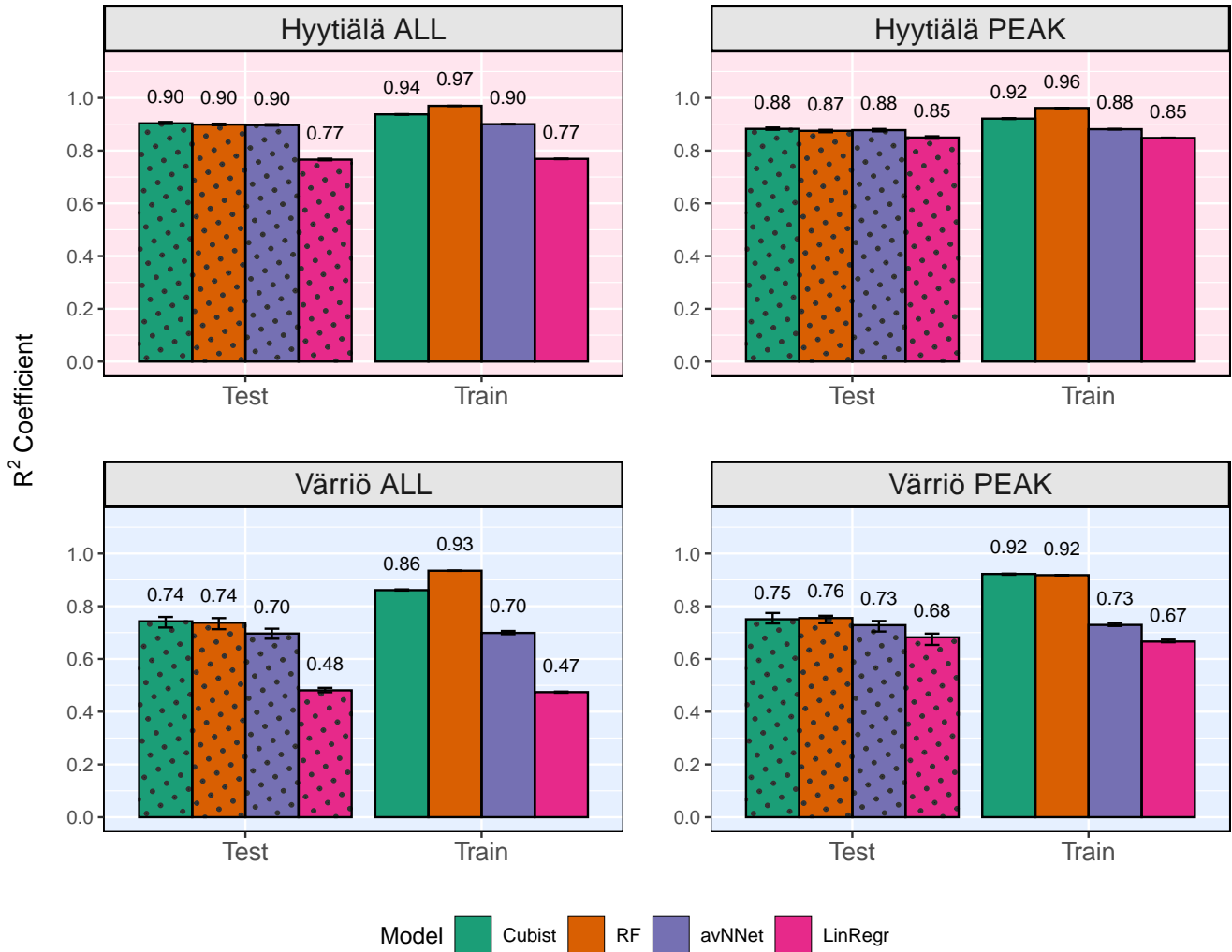


Figure 1. R^2 -coefficients for all [the](#) models and different [data-sets](#) setups from [Set 1 \(Table 3\)](#). In each of the four panels, the results for the training data set are shown on the right (marked 'Train'), and the results for the test data set are shown on the left (dotted bars, marked 'Test'). Different colors are used to distinguish between the ML models, see legend. 'ALL' denotes the scores for the models trained on the whole year data sets; 'PEAK' - for the models trained on the peak growing season data sets. [The black error bars show the min and max, and the bars show the mean of the scores trained on different splits of the data.](#)

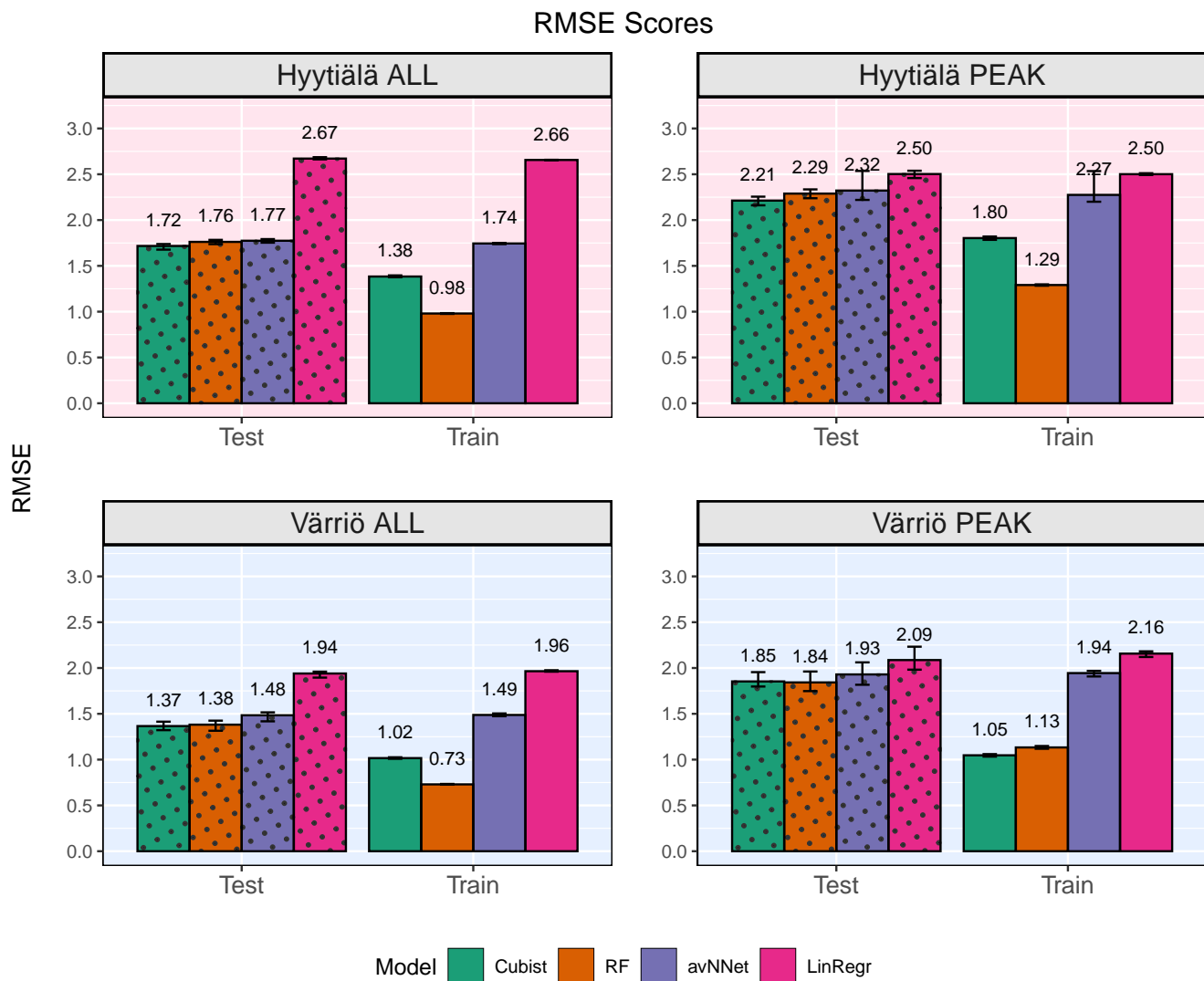


Figure 2. RMSE for all models and different [data-sets](#)[setups from Set 1 \(Table 3\)](#). In each of the four panels, the results for the training data set are shown on the right (marked 'Train'), and the results for the test data set are shown on the left (dotted bars, marked 'Test'). Different colors are used to distinguish between the ML models, see legend. 'ALL' denotes the scores for the models trained on the whole year data sets; 'PEAK' - for the models trained on the peak growing season data sets. [The black error bars show the min and max, and the bars show the mean of the scores trained on different splits of the data.](#)

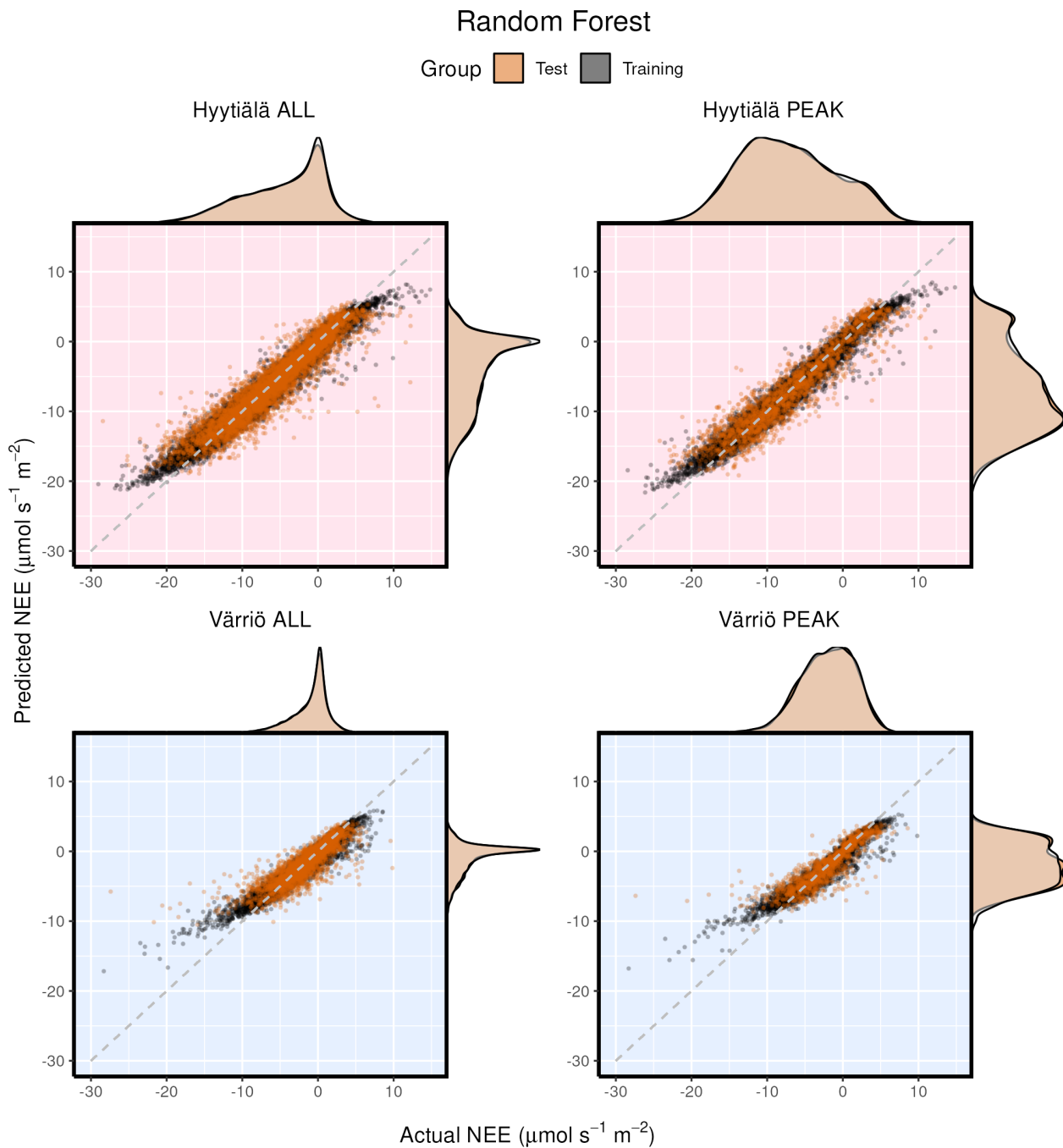


Figure 3. Modelled-Modeled vs measured NEE for Hyttiälä and Värriö on the example of Random Forest model. Black points indicate training data sets, orange - test data sets. 'ALL' denotes the plots based on the whole year data sets; 'PEAK' - on the peak growing season data sets. The density distributions of the actual NEE and predicted NEE are shown on top and right side of the plots, respectively, with colored being the test, and translucent being the training data.

Measured vs. Modeled, Random Forest, Mean and Standard Deviation

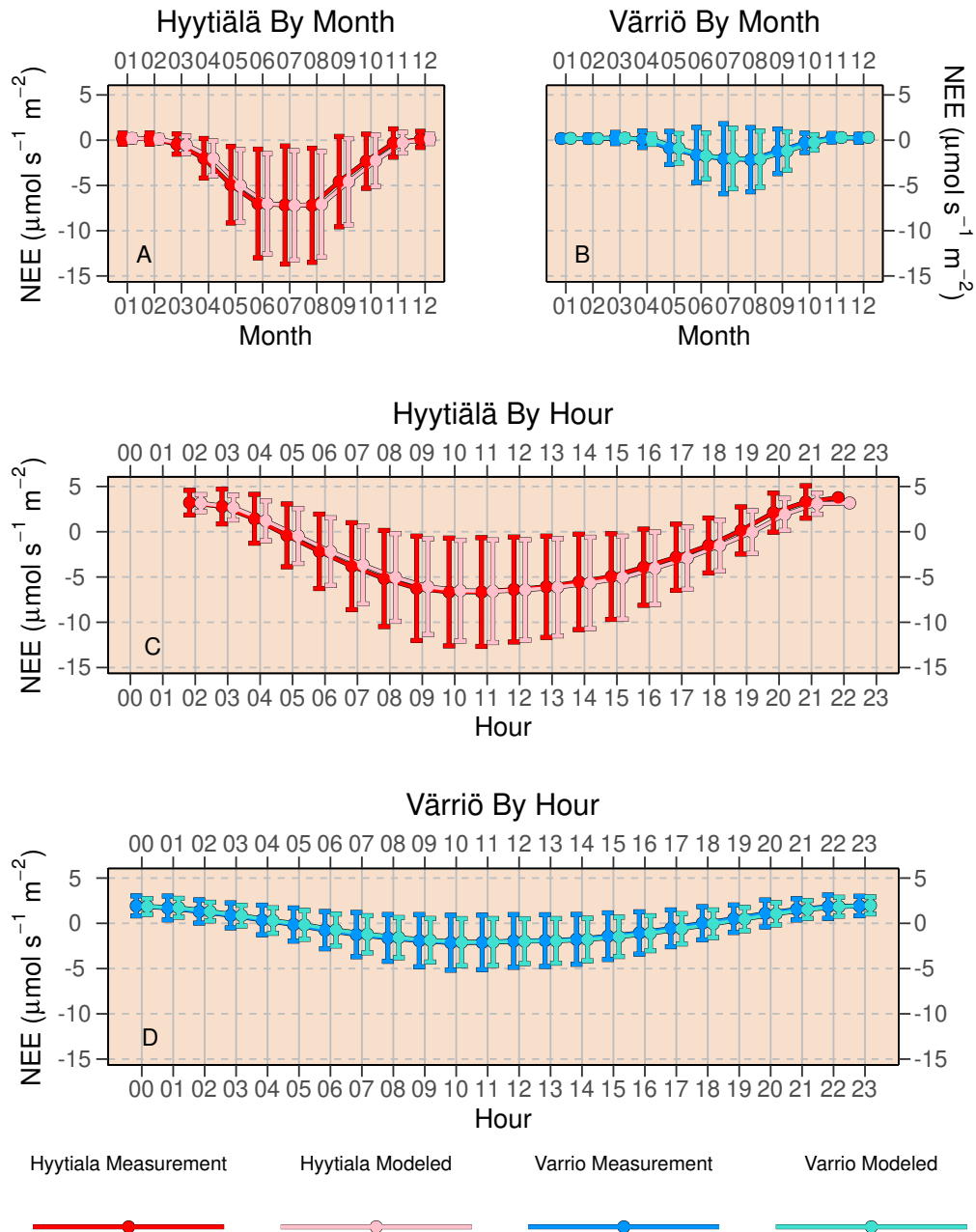


Figure 4. Mean diurnal and monthly cycles of daytime NEE as reproduced by Random Forest compared to actual NEE. Error bars denote standard deviation.

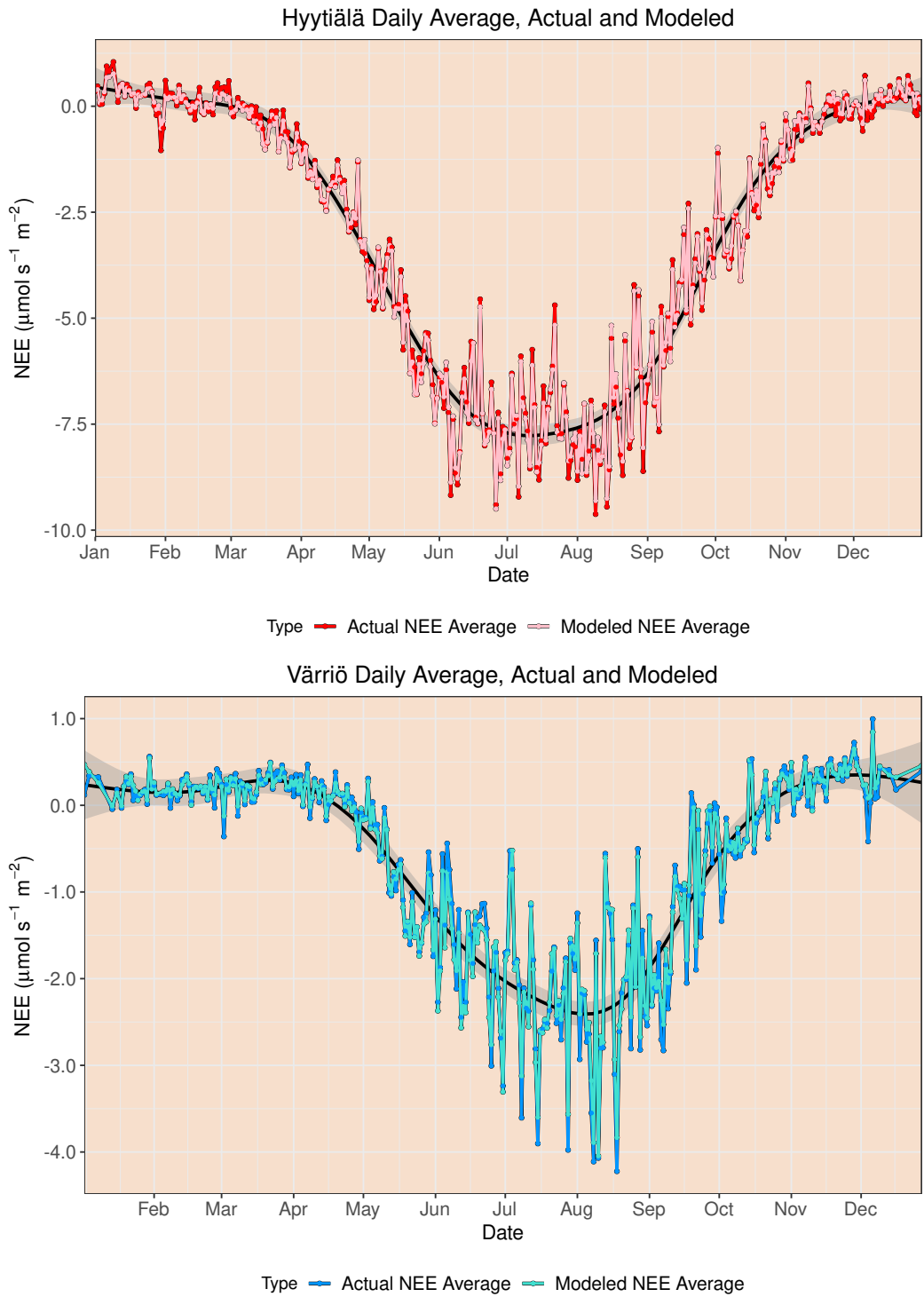


Figure 5. Mean annual cycle of daily NEE as reproduced by Random Forest [compared to actual NEE](#).

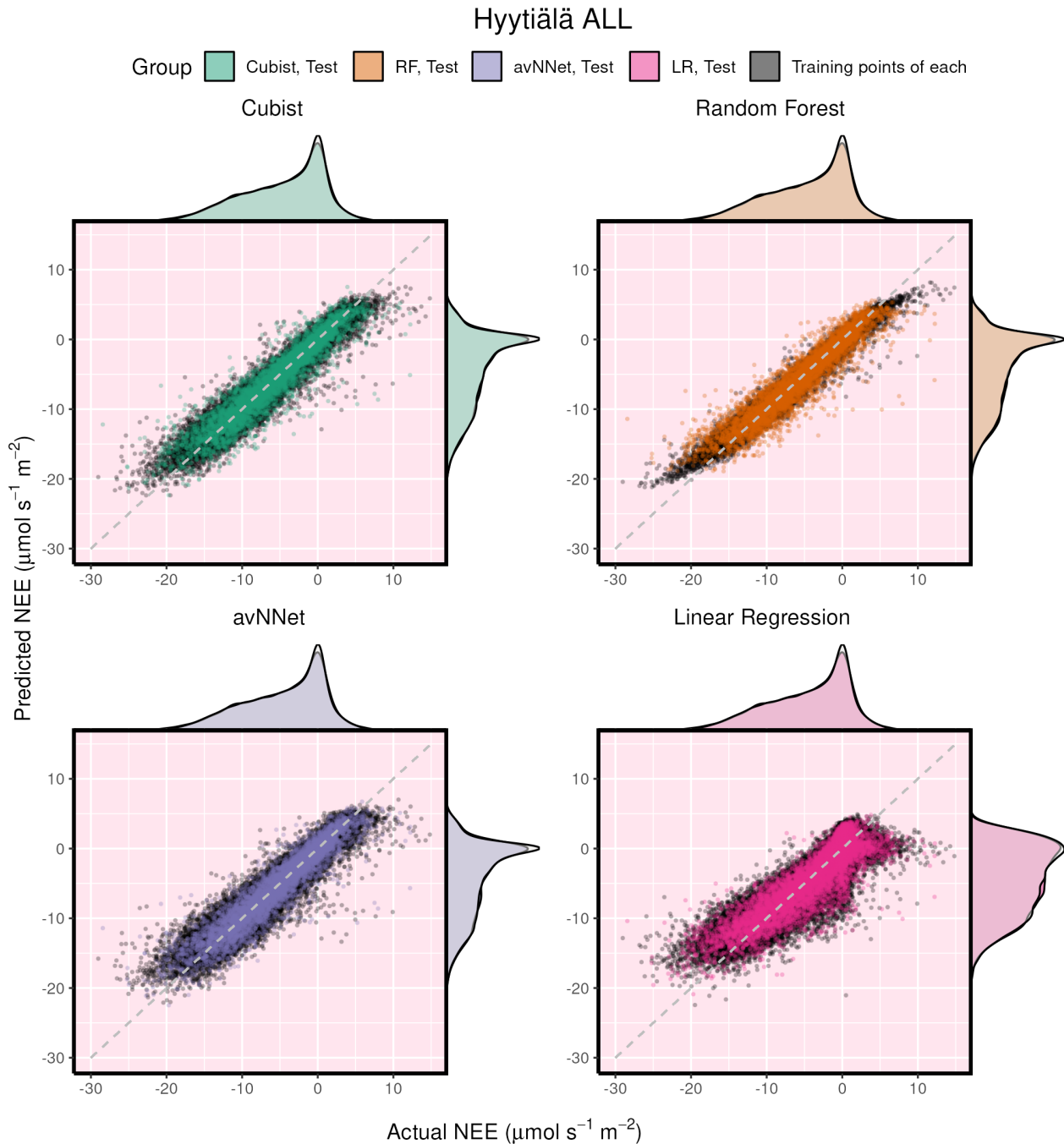


Figure 6. ~~Modelled-Modeled~~ vs measured NEE illustrating performance of all ~~the~~ models on the whole year Hyytiälä data set. Black points indicate ~~the-training~~ data sets ~~used for models'~~, orange - test data sets. ~~The density distributions of the actual NEE and predicted NEE are shown on top and right side of the plots, respectively, with colored being the test, and translucent being the training data.~~

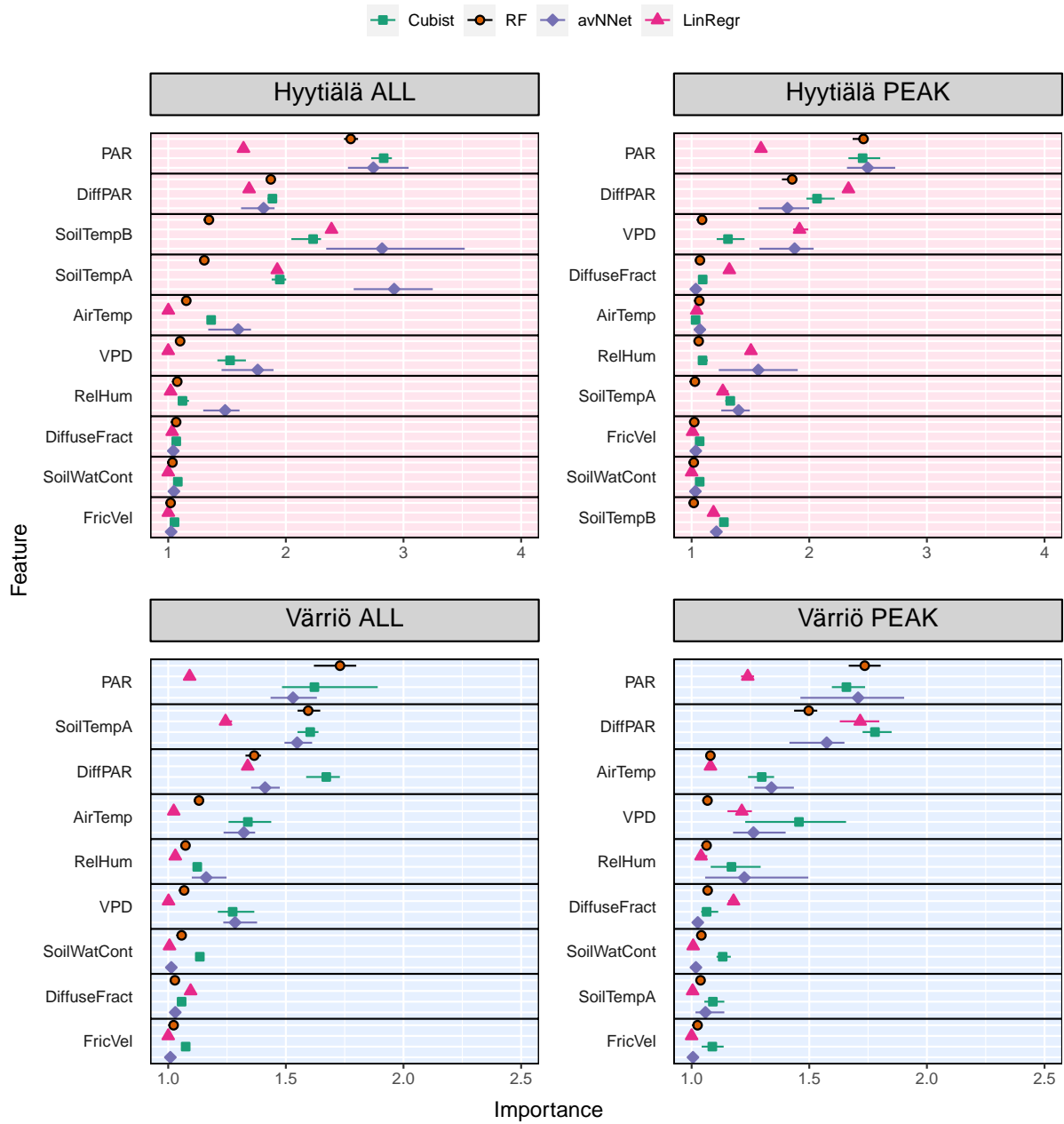


Figure 7. Feature importance for all the models and different data sets setups from Set 1 (Table 3). The order of features is in accordance with the outcome of the Random Forest model. 'ALL' denotes the plots based on the whole year data sets; 'PEAK' - on the peak growing season data sets. The points indicate the mean of the FI score on across multiple datasets, while the bars show the min and max, respectively.

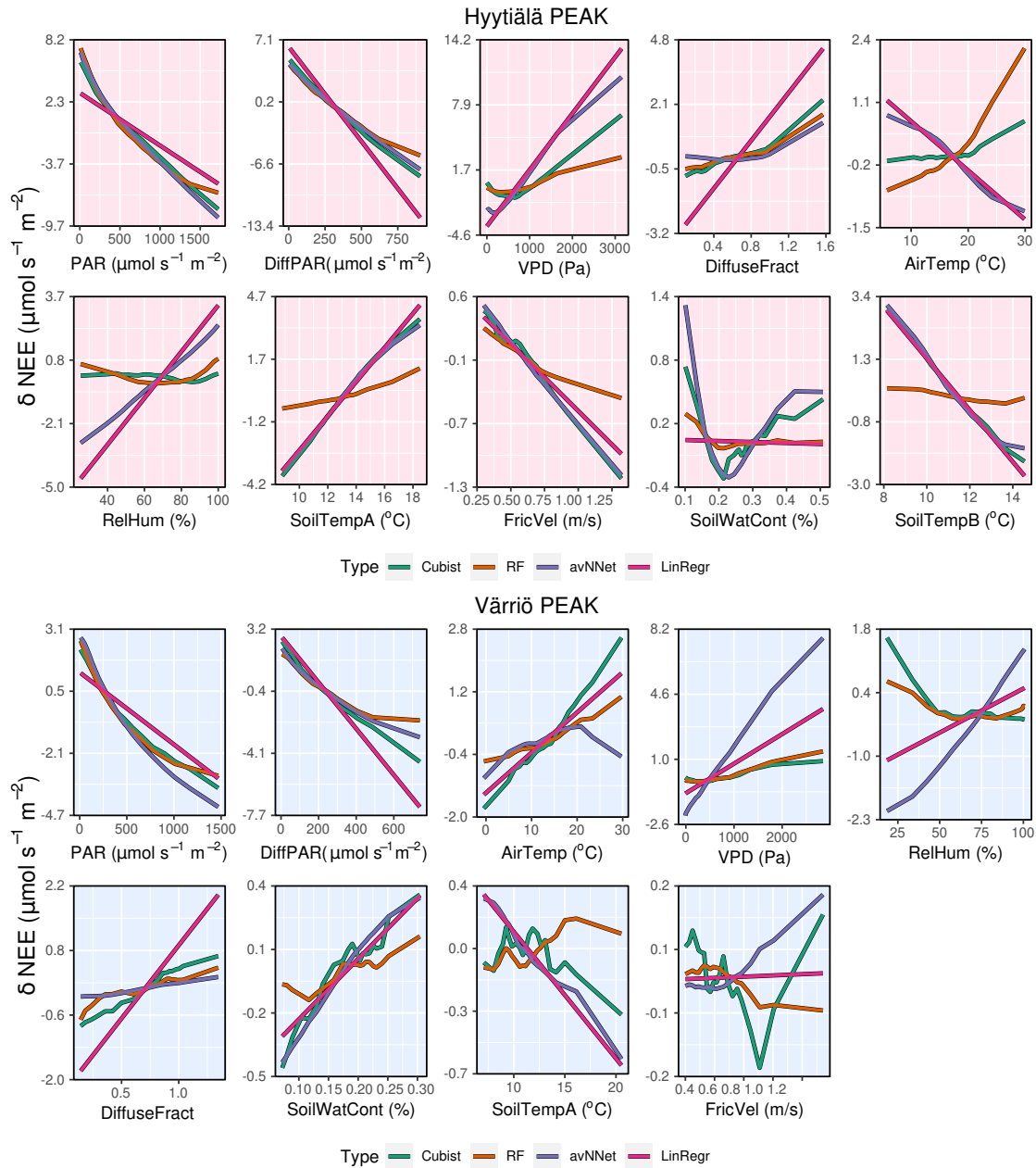


Figure 8. ALE plots for all [the models](#) ([see legend](#)), data sets correspond to the peak growing season in Hyytiälä ([upper panels](#)) and Värriö ([lower panels](#)).

R² Coefficient Scores

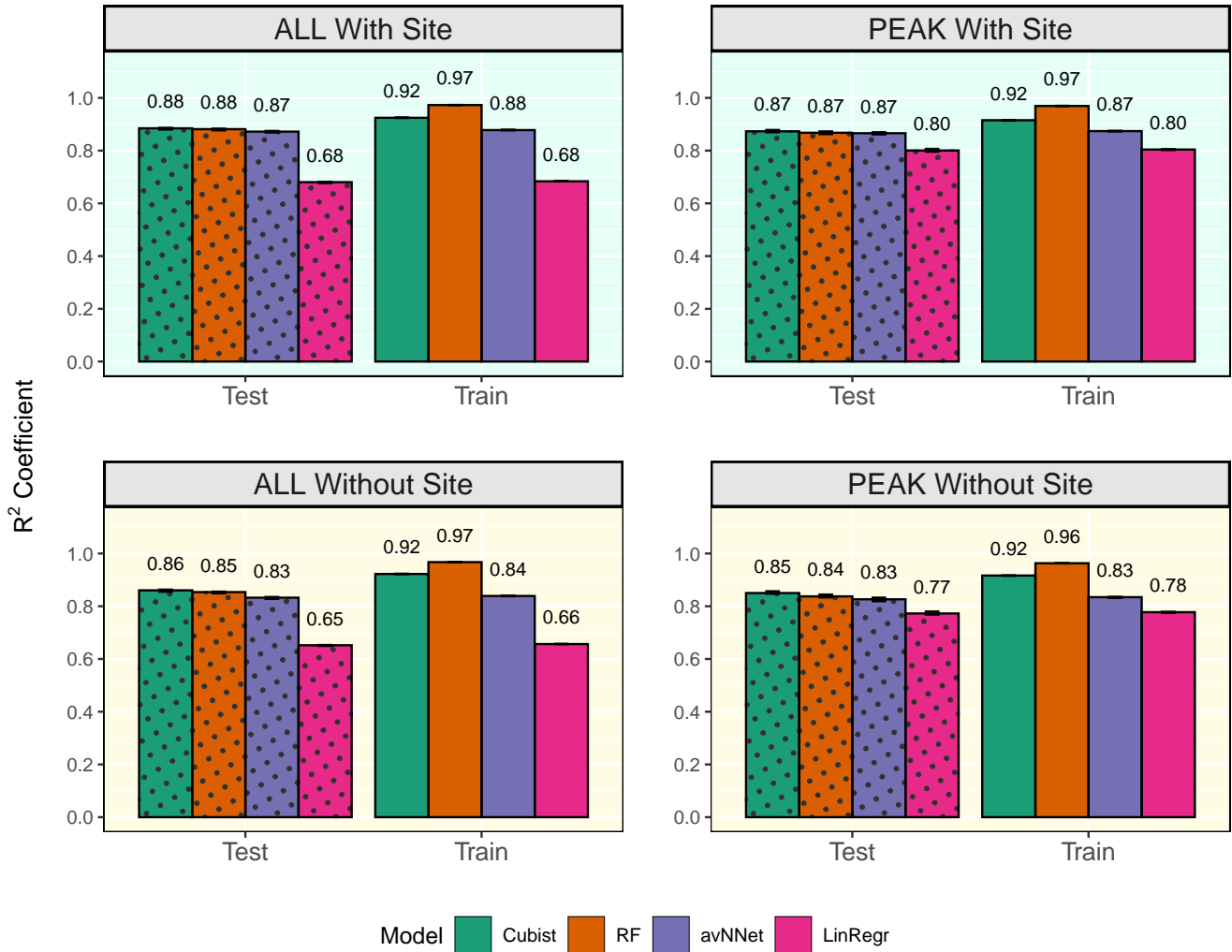


Figure 9. R^2 -coefficients for all [the](#) models and different [data-sets](#) setups from [Set 2 \(Table 3\)](#). In each of the four panels, the results for the training data set are shown on the right (marked 'Train'), and the results for the test data set are shown on the left (dotted bars, marked 'Test'). 'ALL' denotes the scores for the models using the whole year data sets; 'PEAK' - for the models using the peak growing season data sets. 'With Site' - the input variables contain the information about site, 'Without Site' - no information about site. [The black error bars show the min and max, and the bars show the mean of the scores trained on different splits of the data.](#)

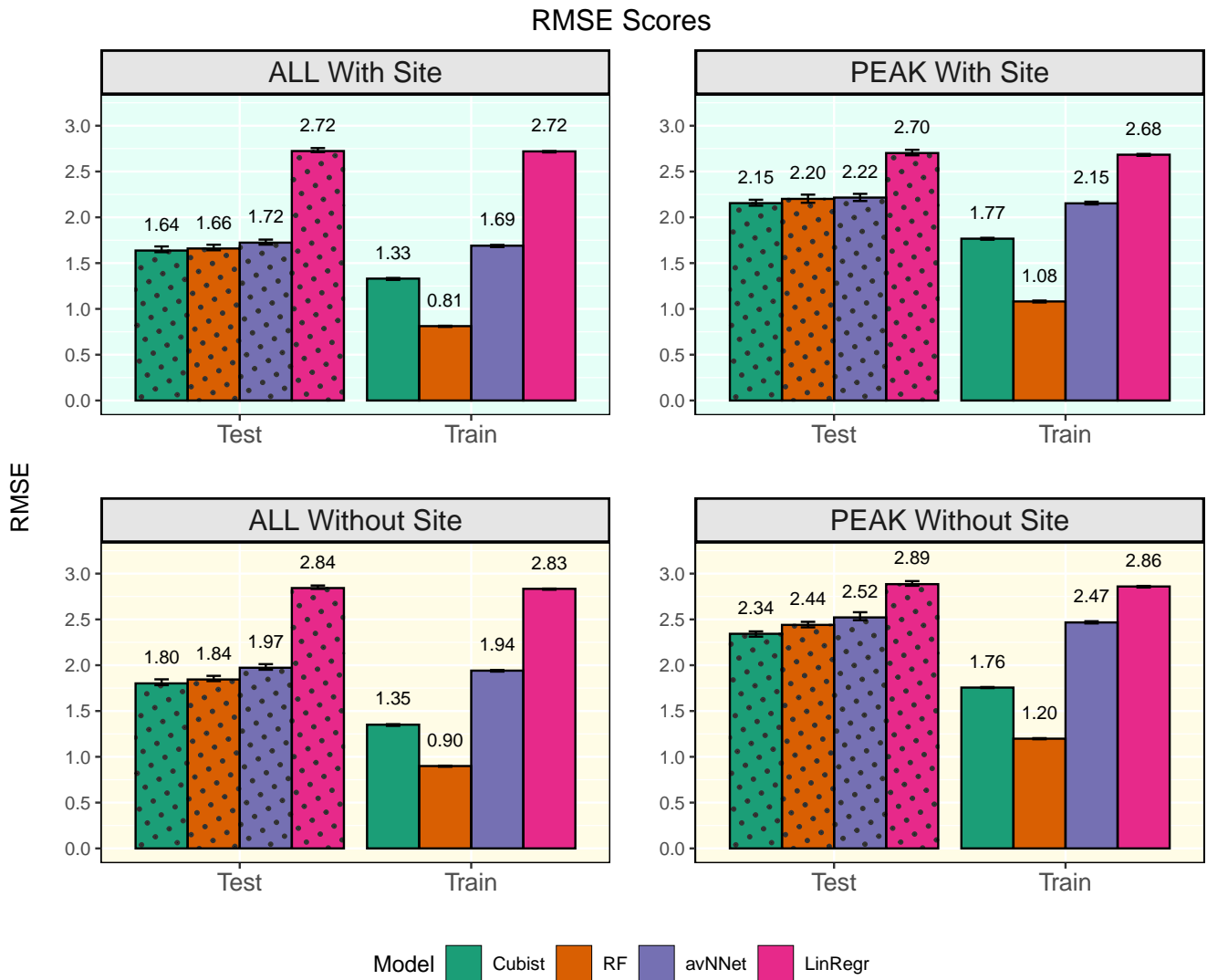


Figure 10. RMSE for all [the](#) models and different [data-sets](#) [setups from Set 2 \(Table 3\)](#). In each of the four panels, the results for the training data set are shown on the right (marked 'Train'), and the results for the test data set are shown on the left (dotted bars, marked 'Test'). 'ALL' denotes the scores for the models using the whole year data sets; 'PEAK' - for the models using the peak growing season data sets. 'With Site' - the input variables contain the information about site, 'Without Site' - no information about site. [The black error bars show the min and max, and the bars show the mean of the scores trained on different splits of the data.](#)

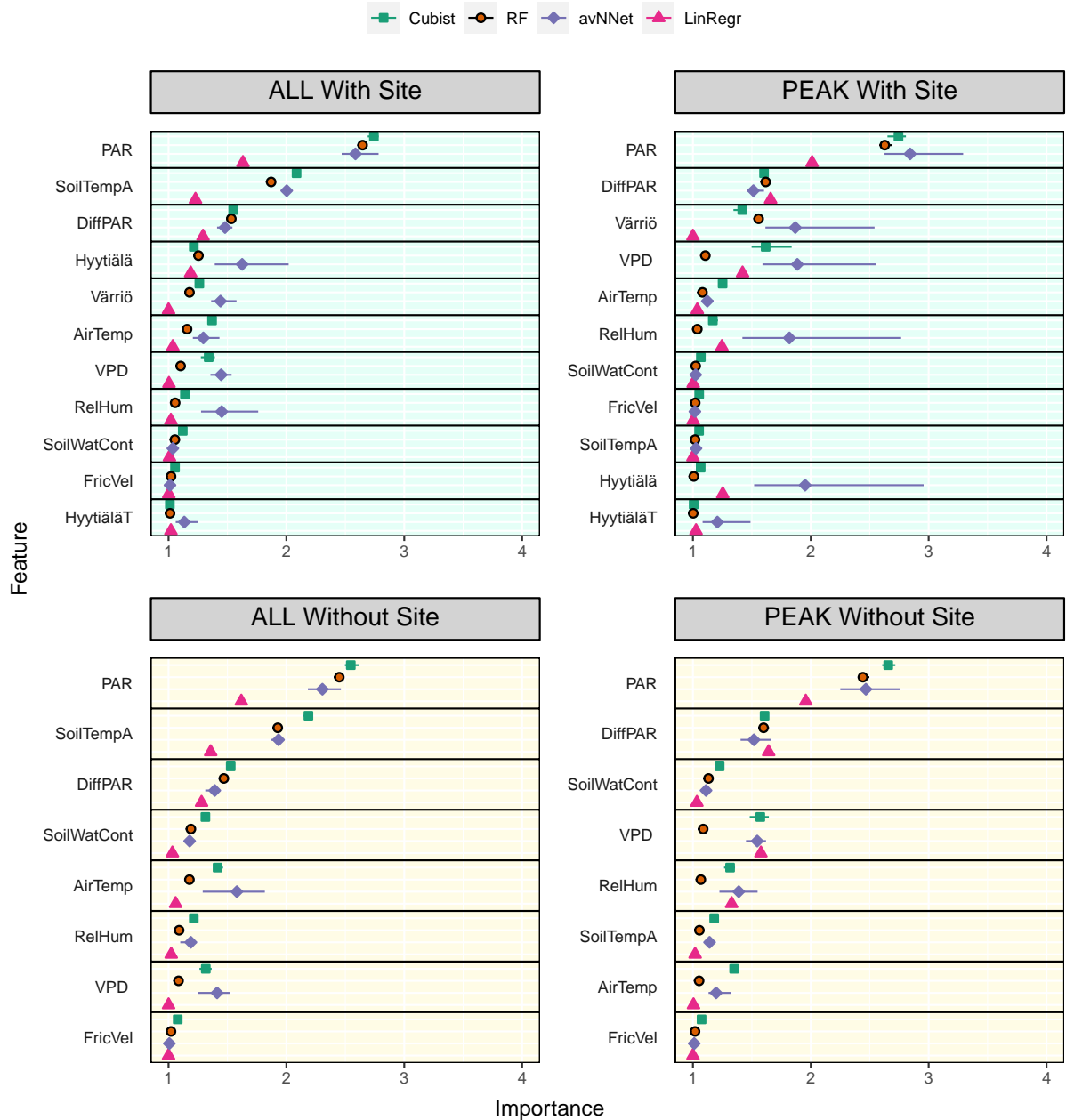


Figure 11. Feature importance for all [the](#) models trained on the mixed data sets containing ('With Site') and not containing ('Without Site') site variables. The order of features is in accordance with the outcome of the Random Forest model. 'ALL' denotes the plots based on the whole year data sets; 'PEAK' - on the peak growing season data sets. [The points indicate the mean of the FI score on across multiple datasets, while the bars show the min and max, respectively.](#)

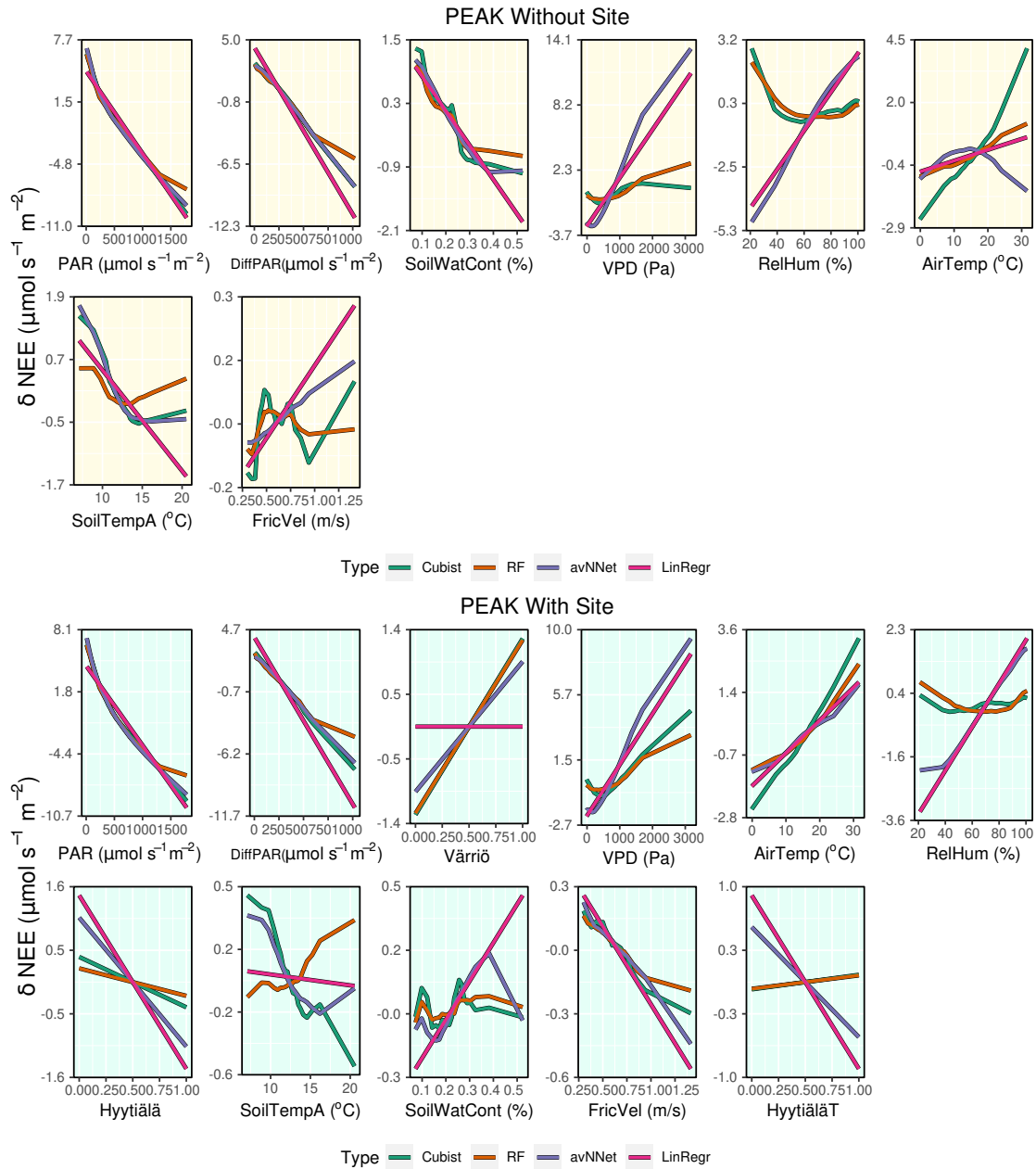


Figure 12. ALE plots for all [the](#) models trained on the mixed data sets containing ('With Site', [lower panels](#)) and not containing ('Without Site', [upper panels](#)) site variables. The data sets are from the peak growing season.

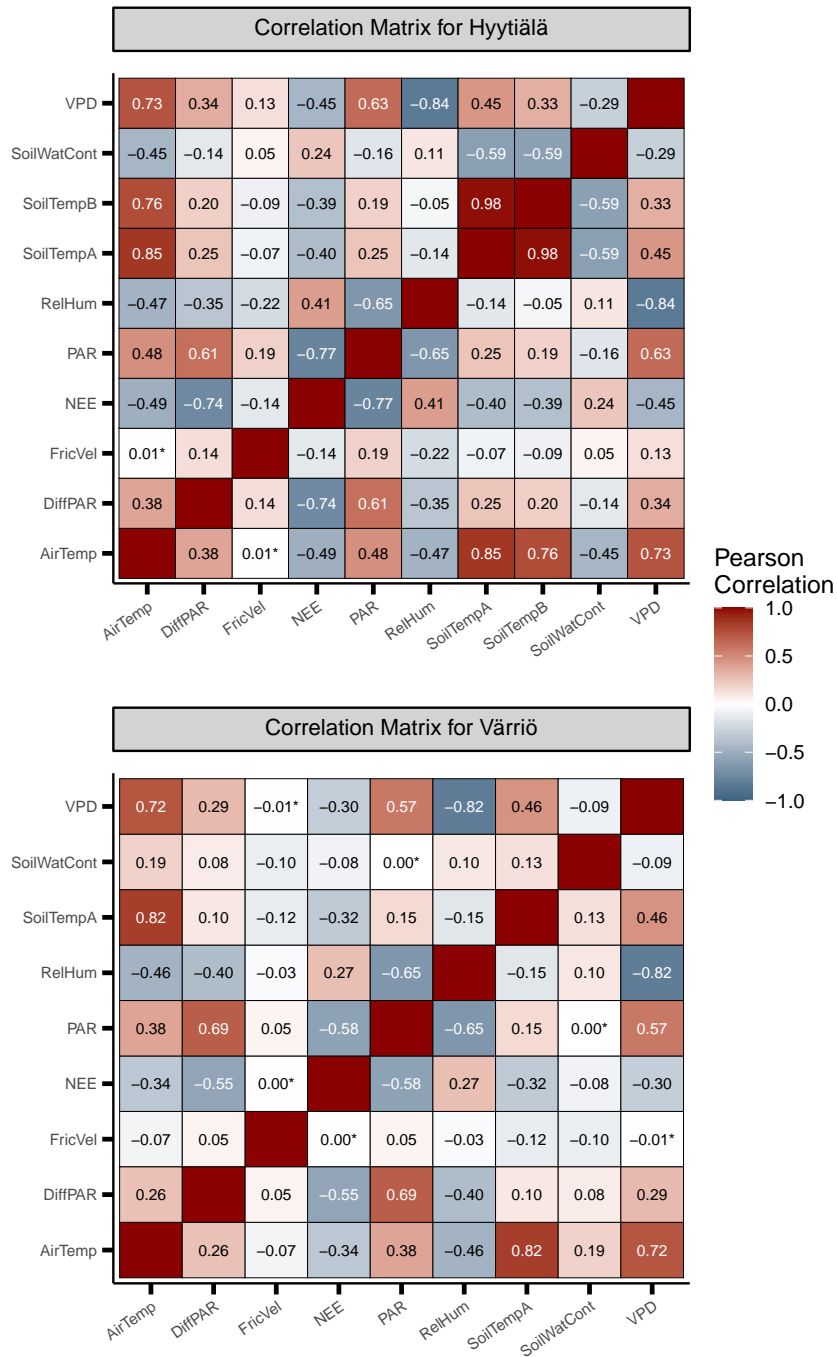


Figure A1. Heat maps illustrating linear correlation between input variables in Hyttiälä and Värriö. Statistically insignificant correlations are marked with *.

Boxplot Representation of Metrics by Site

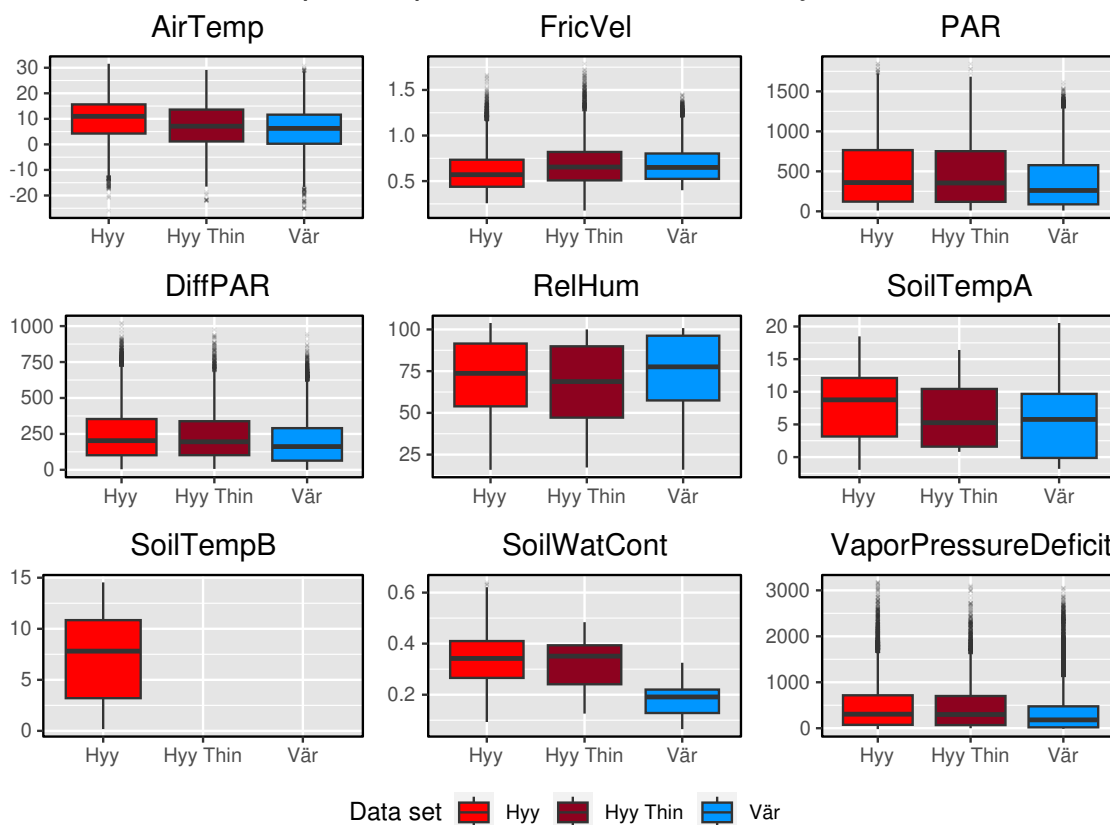


Figure A2. Box plots of input variables comparing Hyttiälä and Värriö data sets [on the whole year time scale](#). 'Hyy' refers to Hyttiälä pre-thinned data set, 'Hyy Thin' - to Hyttiälä post-thinned, 'Vär' - to Värriö data set.

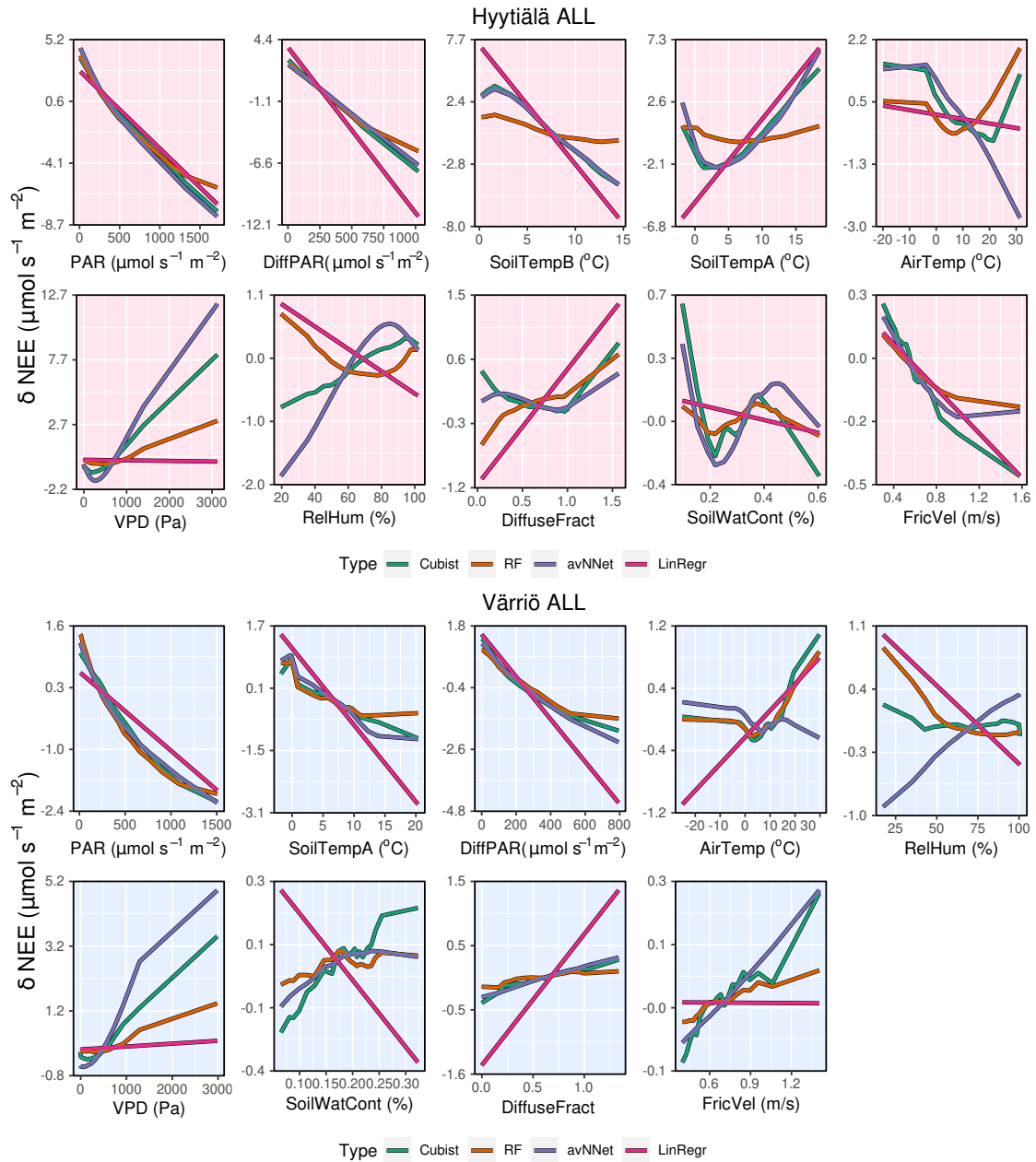


Figure A3. ALE plots for all [the models](#) ~~-, training and test sets contain~~ [trained on the whole-year data sets](#) from [all seasons in](#) Hyttiälä [\(upper panels\)](#) and Värriö [\(lower panels\)](#).

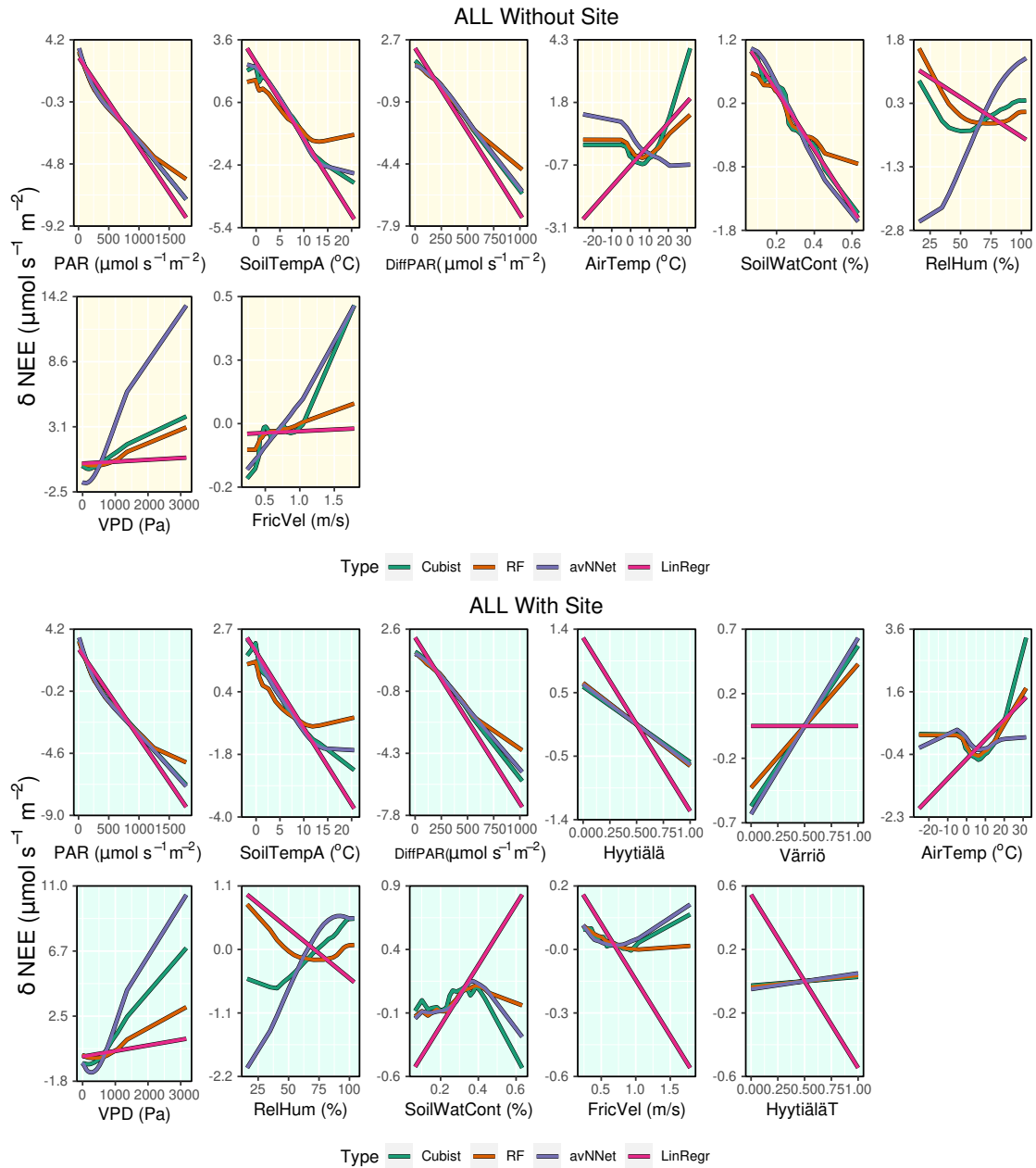


Figure A4. ALE plots for all [the](#) models trained on the mixed data sets containing ('With Site') and not containing ('Without Site') site variables. The [sets contain](#) data [sets are](#) from [all seasons](#) [the whole year](#).

R2 Scores, Balanced Dataset

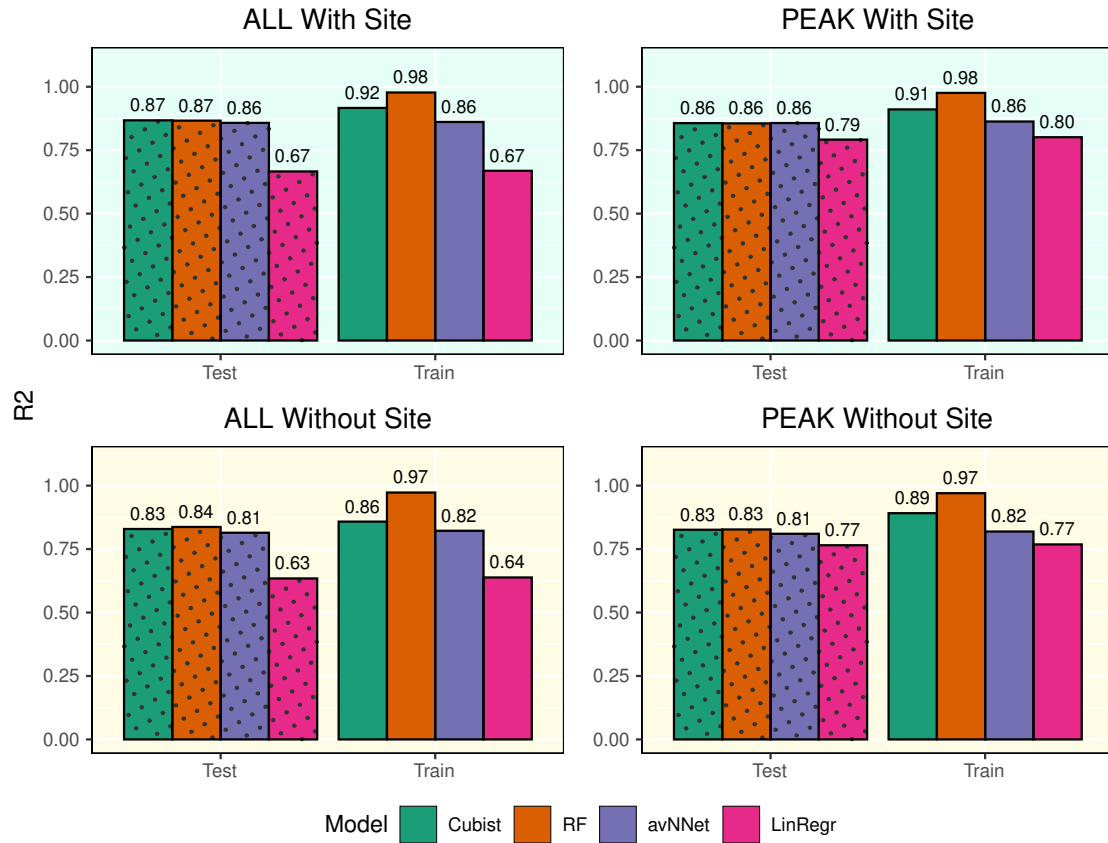


Figure A5. R^2 -coefficients for all the models and different data sets setups from Set 1 (Table 3). Here, the models were trained using equal amount of data points from Hyytiälä, Värriö and post-thinning Hyytiälä (balanced data sets). In each of the four panels, the results for the training data set are shown on the right (marked 'Train'), and the results for the test data set are shown on the left (dotted bars, marked 'Test'). 'ALL' denotes the scores for the models using the whole year data sets; 'PEAK' - for the models using the peak growing season data sets. 'With Site' - the input variables contain the information about site, 'Without Site' - no information about site.

RMSE Scores, Balanced Dataset

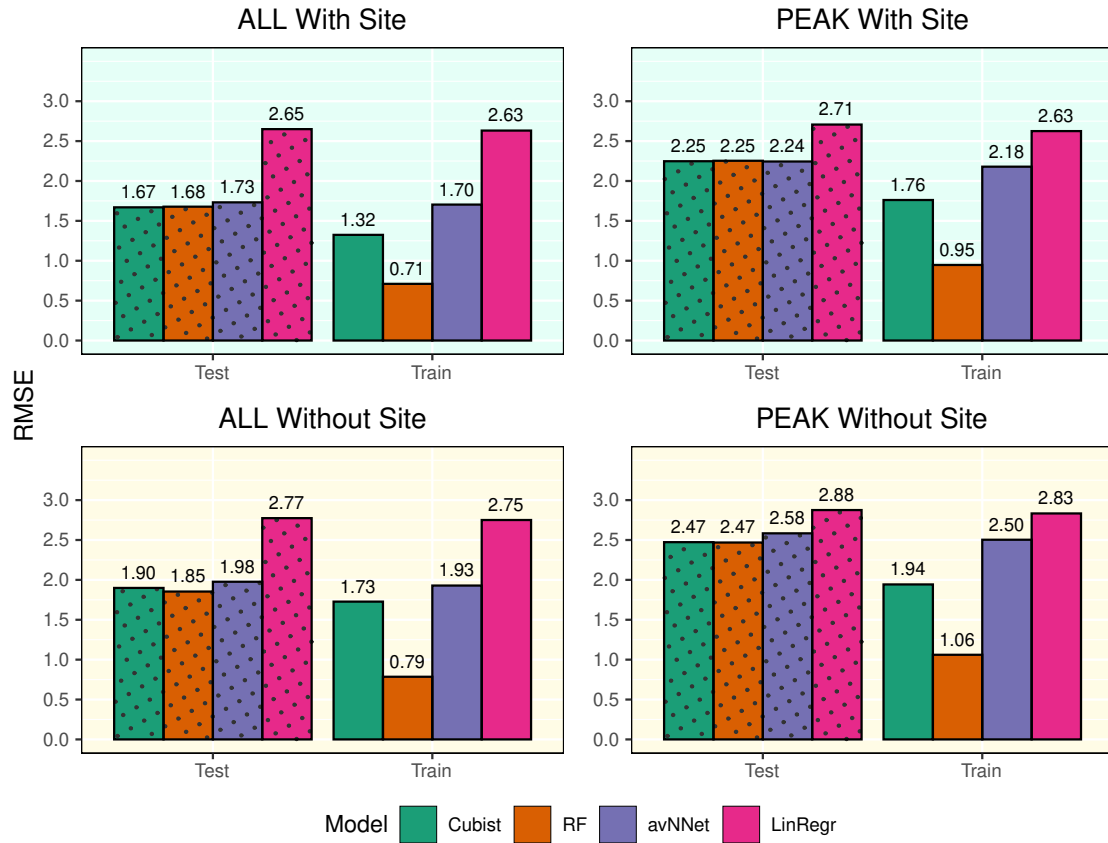


Figure A6. RMSE for all the models using balanced datasets and different setups from Set 1 (Table 3). Here, the models were trained using equal amount of data points from Hyytiälä, Värriö and post-thinning Hyytiälä (balanced data sets). In each of the four panels, the results for the training data set are shown on the right (marked 'Train'), and the results for the test data set are shown on the left (dotted bars, marked 'Test'). 'ALL' denotes the scores for the models using the whole year data sets; 'PEAK' - for the models using the peak growing season data sets. 'With Site' - the input variables contain the information about site, 'Without Site' - no information about site.

Table A1. Three most important features for different models and all-setups Set 1 (Table 3)

Model	RF	Cubist	AvNNNet	LinRegr	RF	Cubist
Peak	Hyytiälä					
P1	PAR	PAR	PAR	DiffR-<u>PAR_{dif}</u>	PAR	DiffR-<u>PAR_{dif}</u>
P2	DiffR-<u>PAR_{dif}</u>	DiffR-<u>PAR_{dif}</u>	DiffR-<u>PAR_{dif}</u>	VPD	DiffR-<u>PAR_{dif}</u>	PAR
P3	VPD	SoiH_A-<u>SoilTemp_A</u>	VPD	PAR	AirT-<u>AirTemp</u>	AirT-<u>AirTemp</u>
All	Hyytiälä					
P1	PAR	PAR	SoiH_B-<u>SoilTemp_B</u>	SoiH_B-<u>SoilTemp_B</u>	PAR	DiffR-<u>PAR_{dif}</u>
P2	DiffR-<u>PAR_{dif}</u>	SoiH_B-<u>SoilTemp_B</u>	PAR	SoiH_A-<u>SoilTemp_A</u>	SoiH_A-<u>SoilTemp_A</u>	SoiH_A-<u>SoilTemp_A</u>
P3	SoiH_B-<u>SoilTemp_B</u>	DiffR-<u>PAR_{dif}</u>	DiffR-<u>PAR_{dif}</u>	DiffR-<u>PAR_{dif}</u>	DiffR-<u>PAR_{dif}</u>	PAR

Table A2. Three most important features for different models and Set 2 (Table 3)

<u>Model</u>	<u>RF</u>	<u>Cubist</u>	<u>AvNNNet</u>	<u>LinRegr</u>	<u>RF</u>	<u>Cubist</u>	<u>AvNNNet</u>	<u>LinRegr</u>
<u>Peak</u>	Without Site				With Site			
<u>P1</u>	<u>PAR</u>	<u>PAR</u>	<u>PAR</u>	<u>PAR</u>	<u>PAR</u>	<u>PAR</u>	<u>PAR</u>	<u>PAR</u>
<u>P2</u>	<u>PAR_{dif}</u>	<u>VPD</u>	<u>PAR_{dif}</u>	<u>PAR_{dif}</u>	<u>PAR_{dif}</u>	<u>PAR_{dif}</u>	<u>VPD</u>	<u>PAR_{dif}</u>
<u>P3</u>	<u>SoilWatCont</u>	<u>PAR_{dif}</u>	<u>VPD</u>	<u>VPD</u>	<u>Värriö</u>	<u>Värriö</u>	<u>PAR_{dif}</u>	<u>VPD</u>
<u>All</u>	Without Site				With Site			
<u>P1</u>	<u>PAR</u>	<u>PAR</u>	<u>PAR</u>	<u>PAR</u>	<u>PAR</u>	<u>PAR</u>	<u>PAR</u>	<u>PAR</u>
<u>P2</u>	<u>SoilTemp_A</u>	<u>SoilTemp_A</u>	<u>SoilTemp_A</u>	<u>SoilTemp_A</u>	<u>SoilTemp_A</u>	<u>SoilTemp_A</u>	<u>SoilTemp_A</u>	<u>PAR_{dif}</u>
<u>P3</u>	<u>PAR_{dif}</u>	<u>PAR_{dif}</u>	<u>AirTemp</u>	<u>PAR_{dif}</u>	<u>PAR_{dif}</u>	<u>PAR_{dif}</u>	<u>VPD</u>	<u>SoilTemp_A</u>